Published for SISSA by Springer

Received: *April 3, 2024*
Revised: *July 6, 2024*
Accepted: *September 30, 2024*
Published: *October 29, 2024*

Measurement of differential ZZ + jets production cross sections in pp collisions at $\sqrt{s} = 13$ TeV

The CMS collaboration

E-mail: cms-publication-committee-chair@cern.ch

Abstract: Diboson production in association with jets is studied in the fully leptonic final states, $\mathrm{pp} \to (\mathrm{Z}/\gamma^*)(\mathrm{Z}/\gamma^*) + \mathrm{jets} \to 2\ell 2\ell' + \mathrm{jets}$, ($\ell, \ell' = \mathrm{e}$ or μ) in proton-proton collisions at a center-of-mass energy of 13 TeV. The data sample corresponds to an integrated luminosity of 138 fb^{-1} collected with the CMS detector at the LHC. Differential distributions and normalized differential cross sections are measured as a function of jet multiplicity, transverse momentum p_T, pseudorapidity η, invariant mass and $\Delta\eta$ of the highest-p_T and second-highest-p_T jets, and as a function of invariant mass of the four-lepton system for events with various jet multiplicities. These differential cross sections are compared with theoretical predictions that mostly agree with the experimental data. However, in a few regions we observe discrepancies between the predicted and measured values. Further improvement of the predictions is required to describe the ZZ+jets production in the whole phase space.

Keywords: Hadron-Hadron Scattering , Vector Boson Production

ArXiv ePrint: 2404.02711

https://doi.org/10.1007/JHEP10(2024)209

JHEP10(2024)209

Contents

1 Introduction **1**

2 The CMS detector **3**

3 Data and Monte Carlo samples **3**

4 Event reconstruction **4**

5 Event selection **6**

6 Background estimates **7**

7 Unfolding and systematic uncertainties **8**

8 Results **12**
- 8.1 Differential distributions 12
- 8.2 Differential cross sections 17

9 Summary **18**

The CMS collaboration **29**

1 Introduction

Measurements of diboson production at the CERN LHC are relevant for precision studies of the standard model (SM). In the SM, ZZ production proceeds mainly through processes represented by the quark-antiquark t- and u-channel scattering diagrams (figure 1 left). In calculations at higher order in quantum chromodynamics (QCD), gluon-gluon fusion also contributes via box diagrams involving quark loops (figure 1 right). The electroweak (EW) and QCD vertices result in the production of Z pairs and of associated jets, and the measurement of this process is the goal of this analysis.

Previously pairs of on-shell Z bosons, produced in the dilepton mass range 60–120 GeV, were studied by the CMS Collaboration using data sets with integrated luminosities of $5.1\,\mathrm{fb}^{-1}$ at $\sqrt{s} = 7\,\mathrm{TeV}$ [1], $19.6\,\mathrm{fb}^{-1}$ at $\sqrt{s} = 8\,\mathrm{TeV}$ [2, 3] in the $\mathrm{ZZ} \to 2\ell 2\ell'$, $\mathrm{ZZ} \to 2\ell 2\tau$ and $\mathrm{ZZ} \to 2\ell 2\nu$ decay channels, where $\ell, \ell' = \mathrm{e}$ or μ, and with integrated luminosities of $2.6\,\mathrm{fb}^{-1}$ [4] and $35.9\,\mathrm{fb}^{-1}$ [5] at $\sqrt{s} = 13\,\mathrm{TeV}$ in the $\mathrm{ZZ} \to 2\ell 2\ell'$ decay channel. The ZZ cross section was also measured at $\sqrt{s} = 5.02\,\mathrm{TeV}$ based on the $\mathrm{ZZ} \to 2\ell 2\ell'$ and $\mathrm{ZZ} \to 2\ell 2\nu$ decay channels [6]. The differential cross sections for Z boson pair production in association with jets were measured at $\sqrt{s} = 8$ and $13\,\mathrm{TeV}$ with integrated luminosities of 19.7 and $35.9\,\mathrm{fb}^{-1}$, respectively, using the $\mathrm{ZZ} \to 2\ell 2\ell'$ decay channel [7]. The most recent measurement of ZZ production cross sections with the full Run 2 data set with an integrated luminosity of $137\,\mathrm{fb}^{-1}$ at $\sqrt{s} = 13\,\mathrm{TeV}$ performed by the CMS Collaboration was published in ref. [8], and

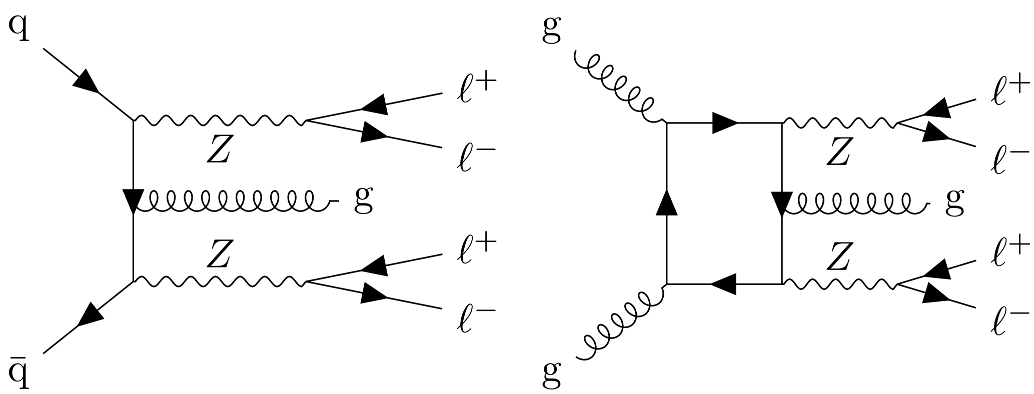

Figure 1. Example Feynman diagrams of ZZ production associated with jets via (left) quark-initiated production and (right) loop-induced gluon fusion production.

results on the EW production of ZZ+2jets were published in ref. [9]. All measurements agree with SM predictions. The ATLAS Collaboration published similar results at $\sqrt{s} = 7$, 8, and 13 TeV [10–15], which also agree with the SM. These measurements are important to test predictions recently made available at next-to-next-to-leading order (NNLO) in QCD [16]. Comparing measurements at the highest collision energies to theoretical predictions tests the ability of the most advanced higher order QCD and EW calculations to predict the cross sections of complex final states with jets and multiple vector bosons, and the full Run 2 proton-proton (pp) collision data at $\sqrt{s} = 13$ TeV allow diboson measurements at the highest energies and integrated luminosities to date.

This paper reports a measurement of the four-lepton production (pp $\rightarrow 2\ell 2\ell'$, where 2ℓ and $2\ell'$ indicate oppositely charged pairs of electrons or muons, and Z/γ^* interference is included) in association with jets at $\sqrt{s} = 13$ TeV using a data set with an integrated luminosity of 138 fb^{-1} recorded in 2016–2018 by the CMS experiment. Cross sections are reported for the nonresonant production of pairs of Z bosons, pp $\rightarrow$ ZZ, in association with jets, where both Z bosons are produced on-shell, defined as Z bosons with mass in the range 60–120 GeV. The effect of the presence of jets on the four-lepton mass ($m_{4\ell}$) distribution is also studied with and without the on-shell requirement. Differential distributions and cross sections are measured with respect to jet multiplicity (N_{jets}), transverse momentum p_T, pseudorapidity η, invariant mass and $\Delta\eta$ of the dijet system composed of the highest-p_T and second-highest-p_T jets, and with respect to $m_{4\ell}$ for events with different jet multiplicities. The results are compared with predictions of theoretical models. This analysis is an extension to that of ref. [8] with a focus on jet variables. The two analyses, ref. [8] and this paper, use the same events with a few minor differences: (i) a 0.3% update in the estimated luminosity of the data set; (ii) the simulation program MadGraph5_aMC@NLO [17] is used instead of POWHEG [18–21] as the nominal $q\bar{q} \rightarrow$ ZZ sample; and (iii) a regularized unfolding method is used instead of a simple matrix inversion. Therefore, the ZZ fiducial cross section measured in ref. [8] is directly valid for this analysis. The results are also compared with recent nNNLO+PS predictions [22, 23], where PS is parton shower.

JHEP10(2024)209

2 The CMS detector

A detailed description of the CMS detector, together with a definition of the coordinate system used and the relevant kinematic variables, can be found in ref. [24].

The central feature of the CMS apparatus is a superconducting solenoid of 6 m internal diameter, providing a magnetic field of 3.8 T. Within the solenoid volume are a silicon pixel and strip tracker, a lead tungstate crystal electromagnetic calorimeter (ECAL), and a brass and scintillator hadron calorimeter, which provide coverage in pseudorapidity $|\eta| < 1.48$ in a cylindrical barrel and $1.48 < |\eta| < 3.00$ in two endcap regions. Forward calorimeters extend the coverage provided by the barrel and endcap detectors to $|\eta| < 5.0$. Muons are detected in gas-ionization detectors embedded in the steel flux-return yoke outside the solenoid in the range $|\eta| < 2.4$, with detection planes made using three technologies: drift tubes, cathode strip chambers, and resistive-plate chambers.

Electron momenta are estimated by combining energy measurements in the ECAL with momentum measurements in the tracker. The momentum resolution for electrons with $p_{\mathrm{T}} \approx 45\,\mathrm{GeV}$ from $\mathrm{Z} \to \mathrm{e}^+\mathrm{e}^-$ decays ranges from 1.7% for nonshowering electrons in the barrel region to 4.5% for showering electrons in the endcaps [25]. Matching muons to tracks identified in the silicon tracker results in a p_{T} resolution for muons with $20 < p_{\mathrm{T}} < 100\,\mathrm{GeV}$ of 1.3–2.0% in the barrel and better than 6% in the endcaps. The p_{T} resolution in the barrel is better than 10% for muons with p_{T} up to 1 TeV [26, 27].

Events of interest are selected using a two-tiered trigger system. The first level, composed of custom hardware processors, uses information from the calorimeters and muon detectors to select events at a rate of around 100 kHz within a fixed latency of 4 μs [28]. The second level, known as the high-level trigger, consists of a farm of processors running a version of the full event reconstruction software optimized for fast processing, and reduces the event rate to around 1 kHz before data storage [29].

3 Data and Monte Carlo samples

The data sample used in this analysis was recorded by the CMS experiment in 2016, 2017, and 2018, corresponding to 36.3, 41.5, and 59.7 fb^{-1} of integrated luminosities, respectively. The details of the luminosity measurement are described in refs. [30–32].

The Monte Carlo (MC) simulation used for this analysis can be divided into signal and background samples. The ZZ signal production via quark-antiquark annihilation is simulated at next-to-leading order (NLO) in QCD with MadGraph5_aMC@NLO v2.4.2 [17] and POWHEG 2.0 [18–21]. The MadGraph5_aMC@NLO sample is used as the nominal $\mathrm{q\bar{q}} \to \mathrm{ZZ}$ sample in reconstruction-level distributions and for unfolding, because this sample is expected to describe data better than POWHEG since it merges the 0-jet and 1-jet NLO processes, whereas the POWHEG sample is simulated at NLO accuracy for 0-jet and LO accuracy for 1-jet processes. The $\mathrm{gg} \to \mathrm{ZZ}$ process is simulated at leading order (LO) with MCFM v7.0 [33]. The cross sections of these samples are normalized to the cross sections calculated at NNLO in QCD for $\mathrm{q\bar{q}} \to \mathrm{ZZ}$ (K factor of 1.1) [16] and at NLO in QCD for $\mathrm{gg} \to \mathrm{ZZ}$ (K factor of 1.7) [34]. The production processes via SM Higgs boson production and decay (specifically $\mathrm{gg} \to \mathrm{H} \to \mathrm{ZZ}$) are simulated with POWHEG at NLO. Electroweak ZZ

JHEP10(2024)209

production in association with two jets is simulated with MadGraph5_aMC@NLO [17] at LO. The nominal SM signal predictions are derived from the MadGraph5_aMC@NLO $q\overline{q} \to ZZ$ sample, the MCFM $gg \to ZZ$ sample, and the MadGraph5_aMC@NLO EW production sample, which includes vector boson fusion Higgs boson contributions and their interference with non-Higgs boson EW production, and the POWHEG $H \to ZZ$ sample.

Simulated events for the irreducible background processes containing four prompt leptons in the final state, such as $t\overline{t}Z$, WWZ, WZZ, and ZZZ, where the last three are combined and denoted as VVV, are simulated with MadGraph5_aMC@NLO at LO ($t\overline{t}Z$) and NLO (VVV).

Parton showering, hadronization and fragmentation are simulated in all samples with PYTHIA 8.226 and 8.230 [35], with parameters set by the CUETP8M1 [36] (CP5 [37]) tune for the 2016 (2017 and 2018) data-taking period, and the NNPDF3.0 (3.1) set of parton distribution functions, PDFs, [38] is used.

Results are also compared with the very recent nNNLO+PS predictions [22, 23], which consist of NNLO predictions for the quark-initiated production combined with parton showers using the $\mathrm{MiNNLO_{PS}}$ method, and NLO predictions for the loop-induced gluon fusion production matched to parton showers, with event generators for the two channels implemented in the POWHEG framework. Spin correlations, interferences, and off-shell effects are included by calculating the full process $pp \to \ell^+\ell^-\ell'^+\ell'^-$ and considering all contributions to the four-lepton final state. The contribution mediated by a Higgs boson is included in the gluon fusion production mode.

As part of the nNNLO+PS predictions, the $q\overline{q} \to ZZ$ predictions from the $\mathrm{MiNNLO_{PS}}$ method are accurate at NNLO for inclusive production and accurate at NLO for Z+1-jet production. The combination of the two jet multiplicities does not require any unphysical merging scale [39]. These predictions are expected to be more accurate at high jet multiplicities than: (i) the POWHEG $q\overline{q} \to ZZ$ predictions, which are accurate at NLO in inclusive production; (ii) the MadGraph5_aMC@NLO predictions, which are simulated at NLO with the 0- and 1-jet processes, and merged using the FxFx scheme [40].

The detector response is simulated using a detailed description of the CMS detector implemented with the Geant4 package [41]. The simulated samples include additional interactions per bunch crossing, referred to as pileup. Simulated events were weighted so that the pileup distribution reproduces that observed in the data.

4 Event reconstruction

Standard CMS reconstruction and identification (ID) algorithms, referred to as particle-flow (PF) [42], are used to reconstruct and identify stable particles arising from collisions — electrons, muons, photons, and charged and neutral hadrons — by combining the signals from all subdetectors. Electrons and muons are considered candidates for the reconstruction of ZZ final states ("signal leptons") if their $p_T^\ell > 7\,(5)$ GeV and their $|\eta^\ell| < 2.5\,(2.4)$ for electrons (muons).

Signal leptons are required to originate from the primary interaction vertex of the event, which is taken to be the vertex corresponding to the hardest scattering in the event, evaluated using tracking information alone, as described in section 9.4.1 of ref. [43]. The distance of the lepton track origin from the primary vertex is required to be <1 cm along the beam line,

JHEP10(2024)209

and <0.5 cm in the transverse plane. Furthermore, the significance of the three-dimensional impact parameter relative to the event vertex, $\mathrm{SIP_{3D}}$, is required to satisfy $\mathrm{SIP_{3D}} \equiv |\frac{\mathrm{IP}}{\sigma_{\mathrm{IP}}}| < 4$ for each lepton, where IP is the distance of closest approach of the lepton track to the primary vertex and σ_{IP} is its associated uncertainty.

Loose and tight ID requirements are defined for each lepton. The tight IDs are used for signal leptons, whereas the loose IDs are used in control regions to define objects that might be spuriously identified as a signal lepton. An electron satisfies the loose ID if it satisfies the p_{T}, η, and vertex requirements above. It satisfies the tight ID if it satisfies the loose ID and the multivariate discriminator described in ref. [44]. A muon satisfies the loose ID if it satisfies the above p_{T}, η, and vertex requirements, and provides a good track-matching between the tracker and the muon detectors. It satisfies the tight ID if it satisfies the loose ID, and either is tagged as a muon by the PF algorithm for the years 2016–2017 (satisfies a multivariate discriminator for the year 2018 [45]), or is a high p_{T} (> 200 GeV) muon and satisfies a set of requirements on the quality of the associated track.

Signal leptons are required to be isolated from other particles in the event. The relative isolation is defined as

$$R_{\mathrm{Iso}} = \left(\sum_{\text{charged}} p_{\mathrm{T}} + \max\left[0, \sum_{\text{neutral}} p_{\mathrm{T}} + \sum_{\text{photons}} p_{\mathrm{T}} - p_{\mathrm{T}}^{\mathrm{PU}}(\ell)\right]\right) \Big/ p_{\mathrm{T}}^{\ell} \tag{4.1}$$

where the sums run over the p_{T} of hadrons and photons in a cone of size $\Delta R \equiv \sqrt{(\Delta\eta)^2 + (\Delta\phi)^2} = 0.3$ around the lepton momentum direction, where ϕ is the azimuthal angle in radians. To mitigate the contribution of pileup interactions to the isolation, charged hadrons are included only if they originate from the primary vertex [46]. The estimated neutral contribution to the isolation from pileup, $p_{\mathrm{T}}^{\mathrm{PU}}(\ell)$, is defined differently for electrons and muons. For electrons, $p_{\mathrm{T}}^{\mathrm{PU}}(\mathrm{e}) \equiv \rho\, A_{\mathrm{eff}}$ where the average p_{T} flow density ρ is calculated for each event using a "jet area" method [47], and is defined as the median of the $p_{\mathrm{T}}^{\mathrm{jet}}/A_{\mathrm{jet}}$ distribution for all pileup jets in the event. The effective area A_{eff} is the geometric area of the isolation cone projection on the face of the calorimeter multiplied by an η-dependent correction factor that accounts for the residual dependence of the isolation value on pileup. For muons, $p_{\mathrm{T}}^{\mathrm{PU}}(\mu) \equiv 0.5 \sum_i p_{\mathrm{T}}^{\mathrm{PU},i}$, where i runs over the momenta of the charged hadron PF candidates originating from pileup vertices, and the factor of 0.5 corrects for the ratio of charged to neutral particles in the isolation cone. For the years 2016–2017, muons are considered isolated if their $R_{\mathrm{Iso}} < 0.35$, whereas for 2018 and for electrons the isolation requirement is included in the multivariate discriminator used for the selection.

The efficiencies for the reconstruction, identification, and isolation of signal leptons are measured in data and simulation using a tag-and-probe technique [48] based on inclusive samples of Z boson events, with an additional sample of J/ψ events for low-p_{T} muons. The measurements are performed in bins of p_{T}^{ℓ} and $|\eta^{\ell}|$, where for electrons the supercluster η is used. The electron selection efficiency in the ECAL barrel (endcaps) varies from ∼85 (77)% at $p_{\mathrm{T}}^{\mathrm{e}} \approx 10$ GeV, to ∼95 (89)% for $p_{\mathrm{T}}^{\mathrm{e}} \geq 20$ GeV, and is ∼85% in the barrel-endcap transition region. The muons are reconstructed and identified with efficiencies above ∼98% within $|\eta^{\mu}| < 2.4$. The ratio between the data and simulation efficiencies in each p_{T}-$|\eta|$ bin is applied as a correction factor to leptons in simulated events. If the correction factor for a given lepton

JHEP10(2024)209

is $f_{\rm eff}^{\ell}(p_{\rm T}{}^{\ell}, \eta^{\ell})$, the efficiency correction for each event is $\prod_{\ell} f_{\rm eff}^{\ell}(p_{\rm T}{}^{\ell}, \eta^{\ell})$, where the product index runs over the four leptons of the ZZ candidate.

Jets are reconstructed based on PF candidates, rejecting the charged hadrons associated to a pileup vertex, with the anti-$k_{\rm T}$ clustering algorithm [49, 50] using a distance parameter $R = 0.4$. To reduce the instrumental background, tight identification criteria based on the multiplicities and energy fractions carried by charged and neutral hadrons are imposed on jets [51]. Jets from pileup are rejected using pileup jet identification criteria based on the compatibility of the associated tracks with the primary vertex, when inside the tracker acceptance, and on the jet topology [46]. Jet energy corrections are applied to the reconstructed jets [52, 53].

5 Event selection

The data samples used in this analysis are selected by the trigger system that requires the presence of a pair of loosely isolated leptons or a triplet of leptons, with minimum-$p_{\rm T}$ thresholds for leptons depending on the lepton combination. Further triggers include a set of single-electron and single-muon triggers, and triggers on leptons of different flavors. The trigger efficiency within the acceptance is greater than 98%.

Events are required to have at least four leptons. Each event should contain at least one lepton with $p_{\rm T} > 20\,{\rm GeV}$, two leptons with $p_{\rm T} > 10\,{\rm GeV}$, and four leptons with $p_{\rm T} > 7\,(5)\,{\rm GeV}$ for electrons (muons). All leptons must pass the "tight" lepton identification and isolation requirements described in section 4.

The leptons are required to be separated by $\Delta R(\ell_1, \ell_2) > 0.02$, and electrons are required to be separated from muons by $\Delta R({\rm e}, \mu) > 0.05$, to remove spurious "ghost" leptons arising from ambiguities in track reconstruction. Lepton pairs originating from hadronic decays are removed by requiring that all oppositely charged lepton pairs in the ZZ candidate have $m_{\ell_1 \ell_2} > 4\,{\rm GeV}$ regardless of lepton flavor.

Z candidates are built from two oppositely-charged leptons of the same flavor. The pair is retained if it satisfies $4 < m_{\ell^+\ell^-} < 120\,{\rm GeV}$. All possible four-lepton candidates in an event are then considered. For each ZZ candidate, the dilepton pair with invariant mass closest to the nominal Z mass $m_{\rm Z}$ (91.1876 GeV [54]) is designated $\rm Z_1$, and the other is designated $\rm Z_2$. The event is kept if $40 < m_{\rm Z_1} < 120\,{\rm GeV}$ and $4 < m_{\rm Z_2} < 120\,{\rm GeV}$.

In the case of multiple ZZ candidates satisfying all requirements, the ambiguity is resolved by selecting the candidate where $m_{\rm Z_1}$ is closest to the nominal Z mass. If more than one lepton combination is still possible, the $\rm Z_2$ candidate is chosen as the one that maximizes the scalar $p_{\rm T}$ sum of the leptons.

In this analysis, the jets are required to have a $p_{\rm T} > 30\,{\rm GeV}$ and $|\eta| < 4.7$. In addition, jets are required to be well separated from any isolated lepton by requiring $\Delta R(\text{jet,lepton}) > 0.4$, where the lepton here satisfies all the tight requirements except for the lower $p_{\rm T}$ requirement ($> 5\,{\rm GeV}$ instead of $> 7\,{\rm GeV}$ for electrons, $> 3\,{\rm GeV}$ instead of $> 5\,{\rm GeV}$ for muons) and a relaxed $\rm SIP_{3D}$ requirement (<10 instead of <4 for electrons).

JHEP10(2024)209

6 Background estimates

The requirement of four well-reconstructed and isolated lepton candidates strongly suppresses any background; therefore, this analysis has very low background contributions, dominated by Z boson and WZ diboson production in association with jets, and $\mathrm{t\bar{t}}$ production.

In a small fraction of cases, particles from jet fragmentation satisfy both lepton identification and isolation criteria, and thus are misidentified as signal leptons. This background is estimated using control data samples. The probability for jets to be misidentified and selected as leptons is measured from a sample of $\mathrm{Z}+\ell_{\text{candidate}}$ events, where Z denotes a pair of oppositely charged, same-flavor leptons that pass the selection requirements and satisfy $|m_{\ell^+\ell^-} - m_{\mathrm{Z}}| < 7\,\text{GeV}$. Each event in this sample must have exactly one additional lepton candidate $\ell_{\text{candidate}}$ that satisfies the loose identification requirements with no isolation requirements applied. The misidentification probability for each lepton flavor, measured in bins of p_{T} and η of the $\ell_{\text{candidate}}$, is defined as the ratio between the number of candidates that pass the final isolation and identification requirements to the total number of candidates in the sample. The number of $\mathrm{Z}+\ell_{\text{candidate}}$ events is corrected for the contamination from WZ production and for ZZ events in which one lepton is not reconstructed. These events have a third genuine, isolated lepton that must be excluded from the misidentification probability calculation. The WZ contamination is suppressed by requiring the missing transverse momentum $p_{\mathrm{T}}^{\text{miss}} < 25\,\text{GeV}$. The $p_{\mathrm{T}}^{\text{miss}}$ is defined as the magnitude of the missing transverse momentum vector $\vec{p}_{\mathrm{T}}^{\text{miss}}$, the projection onto the plane transverse to the beams of the negative vector momentum sum of all reconstructed PF candidates in the event, corrected for the jet energy scale (JES). The transverse mass, calculated as $m_{\mathrm{T}} \equiv \sqrt{(p_{\mathrm{T}}^{\ell} + p_{\mathrm{T}}^{\text{miss}})^2 - (\vec{p}_{\mathrm{T}}^{\ell} + \vec{p}_{\mathrm{T}}^{\text{miss}})^2}$, is required to be $<30\,\text{GeV}$. The residual contribution of WZ and ZZ events, which can be up to a few percent of the $\ell_{\text{candidate}}$ events passing all selection criteria, is estimated from simulation and subtracted.

Two control samples are used to estimate the number of background events in the signal region. Both are defined as samples that contain events with a dilepton candidate satisfying all requirements (as Z_1) and two additional lepton candidates $\ell^+\ell^-$. In one control sample, enriched in WZ+jets events, one ℓ candidate is required to satisfy the tight identification and isolation criteria and the other must fail this selection and instead satisfy only the loose requirements; in the other control sample, enriched in Z+jets events, both ℓ candidates must satisfy the loose criteria, but fail the full criteria. The additional leptons must have opposite charges and the same flavor ($\mathrm{e^{\pm}e^{\mp}}$ and $\mu^{\pm}\mu^{\mp}$). The expected number of background events in the signal region, denoted "Z+X" in the figures, is obtained by scaling the number of observed $\mathrm{Z}_1 + \ell^+\ell^-$ events by the misidentification probability for each lepton failing the selection. The procedure is described in more detail in ref. [55].

In addition to this reducible background, which contributes to approximately 1–2% of the expected $\mathrm{ZZ} \to 2\ell2\ell'$ event yield, the yields from the $\mathrm{t\bar{t}Z}$ and VVV processes with four prompt leptons are estimated from simulated samples to be around 1.0–1.5% of the expected $\mathrm{ZZ} \to 2\ell2\ell'$ yield.

JHEP10(2024)209

7 Unfolding and systematic uncertainties

To obtain differential cross sections normalized to the ZZ fiducial cross sections (for the on-shell ZZ region and for the full four-lepton invariant mass range as defined by the kinematic requirements) and compare CMS data to theoretical predictions, the data are "unfolded" to remove detector resolution, efficiency, and acceptance effects. For each distribution to be unfolded, a response matrix is obtained from simulated signal samples. The response matrix represents the correlation map between the distributions obtained after the full detector simulation, reconstruction, and selection, and the generated distributions they originate from. It is used in unfolding to obtain true physical distributions from observed data. The data are unfolded using the iterative D'Agostini's method [56] including correction for background contributions, with the `RooUnfold` toolkit as described in ref. [57], and compared with the theoretical predictions from MadGraph5_aMC@NLO $q\overline{q} \to$ ZZ and POWHEG $q\overline{q} \to$ ZZ, where MCFM gg $\to$ ZZ, POWHEG H $\to$ ZZ, and MadGraph5_aMC@NLO EW ZZ predictions are also added to these two sets of predictions. The unfolded results are also compared with the nNNLO+PS predictions.

The measured on-shell ZZ fiducial cross section from ref. [8] is $40.5\pm0.7\,(\text{stat})\pm1.1\,(\text{syst})\pm 0.7\,(\text{lumi})$ fb, which agrees well with the expected value of $39.3^{+0.8}_{-0.7} \pm 0.6$ fb. As explained in the introduction, this fiducial cross section is valid for the current analysis. The fiducial phase space selections are similar to the reconstruction-level selections and detailed in table 1. We use the notation m_{Z_1,Z_2} to refer to both m_{Z_1} and m_{Z_2}. The MC particle-level distributions use generator-level leptons "dressed" by adding the momenta of generator-level photons within $\Delta R(\ell,\gamma) < 0.1$ from the direction of the lepton.

In constructing the response matrix, there are MC events that pass the reconstruction-level selections, but do not have corresponding events at particle level that pass the fiducial selections. In the unfolding method used, these out-of-fiducial events are treated as background events that equivalently propagate from an additional particle-level bin to the reconstruction-level bins. The size of the contribution of these out-of-fiducial events can be up to 15% for events with at least one jet. In addition, the nonprompt and VVV background events are also added to the out-of-fiducial events.

The systematic uncertainties are propagated through the unfolding by reevaluating the response matrix with the sample used in building the matrix shifted or reweighted to reflect a one standard deviation variation in the quantity of interest. The resulting difference in the final normalized unfolded distributions is taken as the uncertainty related to that quantity.

The systematic uncertainty in the trigger efficiency is estimated to be 2%, and cancels out in normalized differential cross sections. To evaluate uncertainties associated with lepton efficiencies, the response matrix is reevaluated using lepton efficiency correction factors varied up and down by the tag-and-probe [48] fit uncertainties. Electrons and muons are treated separately, and all leptons of the same type are treated as correlated. For the uncertainties associated with the JES and jet energy resolution, the jet p_T is varied by shifting the JES and the spreading up and down by their uncertainties, and the response matrix is reevaluated.

The uncertainty in lepton fake rates is 40%, and is dominated by the statistical uncertainty but also includes systematic uncertainties associated with the underlying physics processes between events in the 3ℓ and 4ℓ control regions. The reducible background is varied up and

Particle type	Selection
	ZZ base selection
Leptons	$p_{\mathrm{T}}(\ell_1) > 20\,\mathrm{GeV}$ $p_{\mathrm{T}}(\ell_2) > 10\,\mathrm{GeV}$ $p_{\mathrm{T}}(\ell) > 5\,\mathrm{GeV}$ $\lvert\eta(\ell)\rvert < 2.5$
Z and ZZ	$40 < m_{\mathrm{Z}_1} < 120\,\mathrm{GeV}$, $4 < m_{\mathrm{Z}_2} < 120\,\mathrm{GeV}$ $m_{\ell\ell} > 4\,\mathrm{GeV}$ (any oppositely charged same-flavor pair)
Jets	$p_{\mathrm{T}}(\mathrm{j}) > 30\,\mathrm{GeV}$ $\lvert\eta(\mathrm{j})\rvert < 4.7$ $\Delta R(\ell,\mathrm{j}) > 0.4$ for each ℓ,j
	On-shell ZZ region
Z and ZZ	ZZ base selection + $60 < m_{\mathrm{Z}_1,\mathrm{Z}_2} < 120\,\mathrm{GeV}$
	Full $m_{4\ell}$ range
Z and ZZ	ZZ base selection + $m_{4\ell} > 80\,\mathrm{GeV}$

Table 1. Particle-level selections used to define the fiducial phase space.

down by the lepton fake rate uncertainty (40%) and the unfolding is repeated to estimate the associated uncertainty from the difference between the normalized distributions.

The pileup uncertainty is evaluated by recomputing the response matrix with the total inelastic cross section [58], which defines the pileup weights applied to MC, varied up and down by 4.6%. The uncertainty associated with the luminosity is evaluated by reevaluating the response matrix with the simulation normalized to the integrated luminosity varied up and down by its total uncertainty, which is 1.2, 2.3 and 2.5% for 2016, 2017 and 2018, respectively. It is small as expected due to the cancellation from the normalization by the fiducial cross section.

The uncertainty arising from generator-specific modeling differences is evaluated from the difference between the measurements unfolded with the response matrix based on the $\mathrm{q\overline{q}} \to \mathrm{ZZ}$ sample simulated by MadGraph5_aMC@NLO and the POWHEG sample.

The PDF and related strong coupling (α_S) uncertainties are evaluated by reweighting the MadGraph5_aMC@NLO sample to PDF and α_S variations, and then redoing the unfolding and combining the results according to the procedure described in ref. [59]. For the renormalization (μ_R) and factorization (μ_F) scales (QCD scales) uncertainties, the response matrix is reevaluated with the MadGraph5_aMC@NLO $\mathrm{q\overline{q}} \to \mathrm{ZZ}$ sample reweighted to reflect the distribution with μ_F and μ_R independently varied up and down by a factor of

JHEP10(2024)209

Systematic source	Uncertainty range
Electron efficiency	0.13–0.30%
Muon efficiency	0.02–0.08%
Jet energy resolution	1.65–3.85%
JES correction	0.93–5.32%
Reducible background	0.05–0.43%
Pileup	0.04–1.08%
Luminosity	$< 0.03\%$
$q\overline{q} \rightarrow ZZ$ MC choice	0.52–4.52%
$gg \rightarrow ZZ$ cross section	0.01–0.19%
QCD scales	0.16–0.82%
PDF	0.05–0.12%
PDF α_S	0.01–0.10%

Table 2. Contributions of each source of systematic uncertainty to the normalized differential cross section measurements of jet variables. Uncertainties depend on the distributions and are listed as a range.

2. All combinations are considered except those in which μ_F and μ_R differ by a factor of four, and the envelope of all variations is used.

The normalization of the MCFM sample ($gg \rightarrow ZZ$) is varied by the scale and PDF uncertainties of its cross section ($^{+18\%}_{-14\%}$), and the resulting difference between the normalized distributions is used.

The contributions of each source of systematic uncertainty to the final results are summarized in tables 2–4. The numbers in these tables are only indicative. They are estimated by varying each source and obtaining the difference in the normalized unfolded distributions. Each number in the tables is not showing an estimate of uncertainty per bin, but an estimate of the portion of the uncertainty contribution per distribution, given by

$$\frac{\sum_{i=1}^{N_{\text{bins}}} |h_{\text{central}}(i) - h_{\text{varied}}(i)|}{\sum_{i=1}^{N_{\text{bins}}} h_{\text{central}}(i)} \tag{7.1}$$

where h_{central} and h_{varied} are the central and varied histograms, respectively, both with sum of bin contents normalized to 1, and N_{bins} is the total number of bins. There are, in general, two estimates from up/down variations and the larger one is used.

JHEP10(2024)209

Systematic source	$m_{4\ell}$ with all jets	0 jet	1 jet	2 jets	3 and more jets
Electron efficiency	0.42%	0.38%	0.66%	0.36%	0.26%
Muon efficiency	0.05%	0.06%	0.07%	0.09%	0.08%
Jet energy resolution	—	0.07%	1.72%	1.65%	0.80%
JES correction	—	0.17%	1.77%	1.95%	0.97%
Reducible background	0.18%	0.18%	0.32%	0.33%	0.96%
Pileup	0.02%	0.05%	0.11%	0.13%	0.35%
Luminosity	0.01%	0.01%	0.02%	0.02%	0.05%
$q\overline{q} \rightarrow ZZ$ MC choice	0.35%	0.65%	0.94%	0.48%	0.35%
$gg \rightarrow ZZ$ cross section	0.02%	0.03%	0.09%	0.06%	0.09%
QCD scales	0.15%	0.16%	0.58%	0.54%	0.62%
PDF	0.05%	0.05%	0.15%	0.15%	0.21%
PDF α_S	0.02%	0.01%	0.05%	0.03%	0.02%

Table 3. The contributions of each source of systematic uncertainty in the normalized differential cross sections measurements as a function of $m_{4\ell}$ with jet multiplicity from 0 to 3 and more, in events satisfying $60 < m_{Z_1,Z_2} < 120\,\text{GeV}$.

Systematic source	$m_{4\ell}$ with all jets	0 jet	1 jet	2 jets	3 and more jets
Electron efficiency	2.12%	2.55%	2.28%	1.77%	1.46%
Muon efficiency	0.71%	0.78%	0.92%	0.79%	0.42%
Jet energy resolution	—	0.11%	1.73%	2.63%	2.32%
JES correction	—	0.33%	1.64%	3.01%	2.02%
Reducible background	2.22%	2.19%	2.88%	3.40%	5.09%
Pileup	0.21%	0.28%	0.19%	0.32%	0.52%
Luminosity	0.12%	0.12%	0.16%	0.17%	0.25%
$q\overline{q} \rightarrow ZZ$ MC choice	0.57%	0.48%	1.22%	3.07%	4.21%
$gg \rightarrow ZZ$ cross section	0.10%	0.18%	0.61%	0.80%	0.46%
QCD scales	0.27%	0.25%	0.67%	1.25%	1.86%
PDF	0.07%	0.09%	0.20%	0.23%	0.28%
PDF α_S	0.08%	0.08%	0.15%	0.20%	0.28%

Table 4. The contributions of each source of systematic uncertainty in the normalized differential cross sections measurements as a function of $m_{4\ell}$ with jet multiplicity from 0 to 3 and more, in events from the full $m_{4\ell}$ range.

JHEP10(2024)209

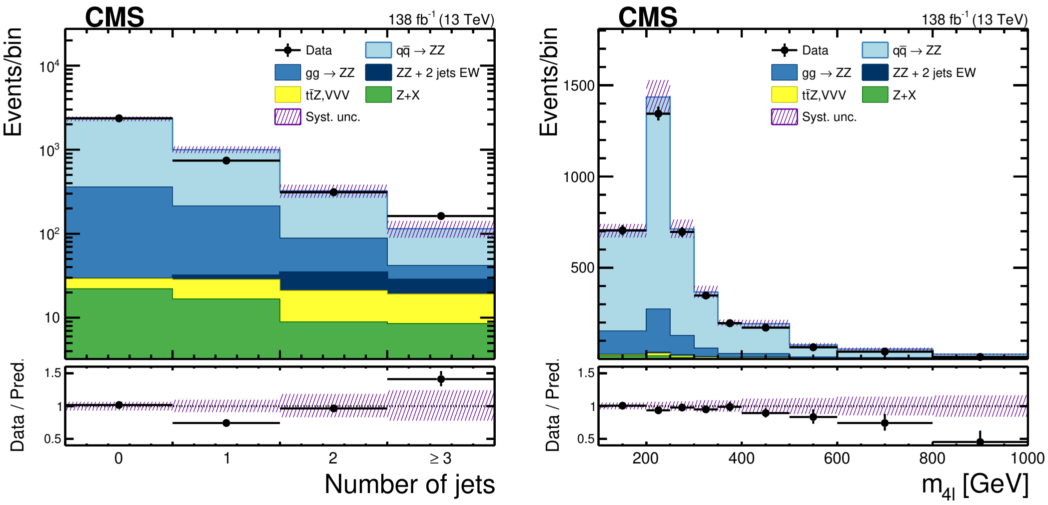

Figure 2. Distribution of the number of jets with $p_T > 30$ GeV (left) and of m_{ZZ} (right) for ZZ+jets events with $60 < m_{Z_1,Z_2} < 120$ GeV for the combined 4e, 4μ, and 2e2μ decay channels. Points represent the data, vertical bars the statistical uncertainties, and shaded histograms represent the expected standard model predictions and reducible background estimated from data. The purple band of slashes represents the systematic uncertainties in the predictions, which includes systematic uncertainties associated with trigger efficiency, lepton efficiencies, jet energy correction and jet energy resolution, pileup, luminosity, Monte Carlo generator choice, $gg \to ZZ$ cross section, and reducible background. The overflow is included in the last bin of the distributions.

8 Results

8.1 Differential distributions

Differential distributions for various reconstructed quantities are presented in this subsection. We proceed with unfolding the data to compare directly with particle-level theoretical predictions, and the results are presented in the next subsection. Figure 2 (left) shows the number of reconstructed jets with $p_T > 30$ GeV for the ZZ+jets events with $60 < m_{Z_1,Z_2} < 120$ GeV. The last bin includes all events with three or more jets. The description of events with three and more jets requires NNLO and even higher corrections, but there are not enough hard jets from the matrix element in the MC samples used, therefore the difference between data and predictions at high jets multiplicity is expected. The 0 and 2 jet bins are well described by the predictions, whereas in the 1 jet bin the predictions significantly overestimate the measured event yield. The $m_{4\ell}$ distribution is shown in figure 2 (right), inclusive in the number of jets. This distribution is well described by the predictions, except for the increasing discrepancy between data and MC towards high masses; this can be mitigated by adding the EW corrections, as demonstrated in ref. [22] and in the next subsection.

Figure 3 shows the p_T and $|\eta|$ distributions for the highest- and second-highest-p_T jet in events with at least one and two jets, respectively. As expected from the distribution of the number of jets, the predictions overestimate the measurements in the highest-p_T jet distributions. The largest difference is observed for highest-p_T jets with $p_T < 100$ GeV, whereas the second-highest-p_T distributions are better described. Apart from the difference

JHEP10(2024)209

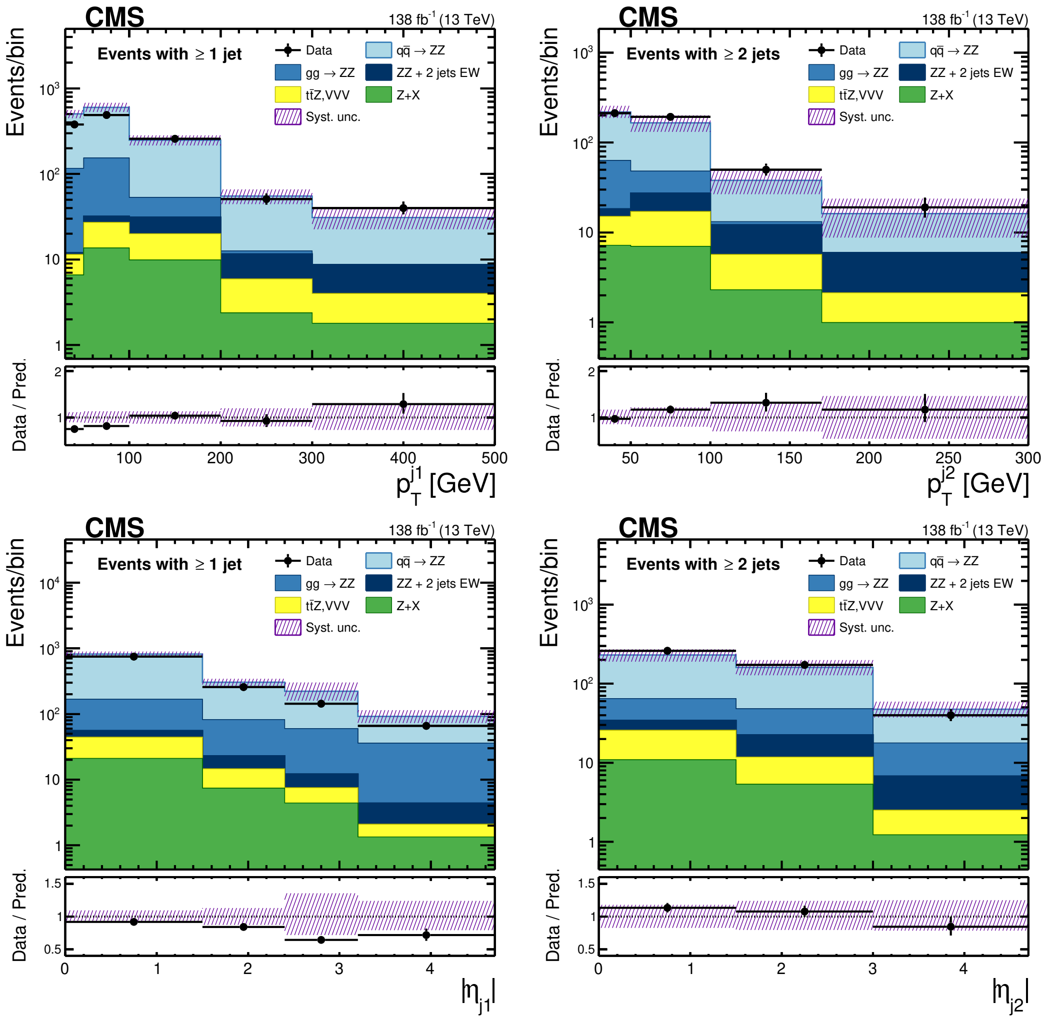

Figure 3. Distribution of the p_T of the highest-p_T jet (upper left) in events with at least one jet, and of the p_T of the second-highest-p_T jet (upper right) in events containing at least two jets. The $|\eta|$ distribution of the highest-p_T (lower left) and second-highest-p_T (lower right) jets. Events are required to have $60 < m_{Z_1,Z_2} < 120\,\text{GeV}$. Other details are as in the caption of figure 2.

in the yield, the p_T distributions of both the highest-p_T and second-highest-p_T jets show similar differential behavior with respect to the predictions (similar trend up to 300 GeV), which is demonstrated in the lower panels of the figures, where data-to-prediction ratios are presented. Similar conclusions are valid also for the $|\eta|$ distributions.

The invariant mass of the dijet system and $\Delta\eta$ between two jets with highest p_T are among the most important dijet distributions. The dijet mass distribution is well described by predictions, as shown in figure 4 (left), whereas in the $|\Delta\eta|$ distribution there is a small trend between data and predictions that can be seen in the lower panel of figure 4 (right). As expected, the contribution of the EW ZZ production is increasing towards the high jet separation and dijet mass, but still remains a small part of the total ZZ cross section.

The effect of the presence of jets in ZZ events is also studied using the $m_{4\ell}$ distribution for different jet multiplicities (figures 5, 6). Each distribution contains only events with exactly

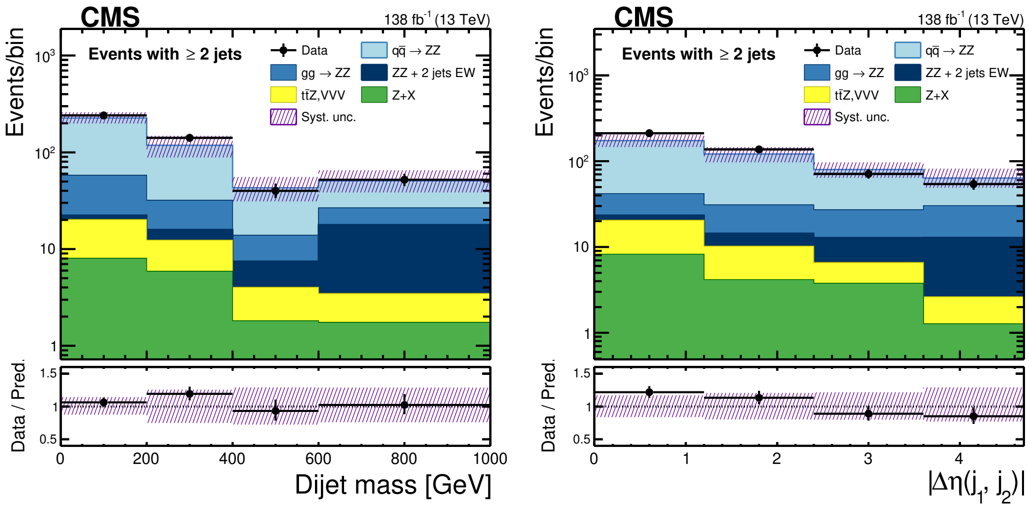

Figure 4. The dijet mass (left) and $|\Delta\eta|$ (right) between the two highest-p_T jets in events with at least two jets. Events are required to have $60 < m_{Z_1,Z_2} < 120$ GeV. Other details are as in the caption of figure 2.

0, 1, 2, 3 jets or ≥4 jets. The predictions describe well the normalized differential behavior, but fail to describe the event yield in the 1-jet case. With increasing jet multiplicities the predicted yields decrease much faster than the measured ones. In the case of 4 or more jets, the data yields are significantly larger than predicted. All distributions in figure 5 are presented for events with on-shell Z bosons, $60 < m_{Z_1,Z_2} < 120$ GeV.

The same analysis is repeated in the full $m_{4\ell}$ range and the results are presented in figure 6. The data and MC predictions are compared in three mass regions: Z boson region, Higgs boson region, and nonresonant ZZ production region. It is important to note that the Higgs boson sample is simulated using the POWHEG NLO predictions, whereas a similar contribution in the ZZ sample has the $gg \to ZZ$ process simulated at LO and normalized to NLO prediction (see section 3 for detail). As shown in figure 6 (upper left), the predictions describe well the data that are inclusive in jet multiplicity. In figure 6 (middle left), the predictions do not describe the event yield of the ZZ nonresonant part, but agree well with data in the Z and Higgs boson production regions. With increasing jet multiplicity, the agreement between data and predictions for ZZ and Z production regions becomes worse, whereas the predictions for the Higgs boson region are compatible with the data within large statistical uncertainties.

The measured and expected event yields for all decay channels and jet multiplicities in different mass ranges are summarized in tables 5 and 6.

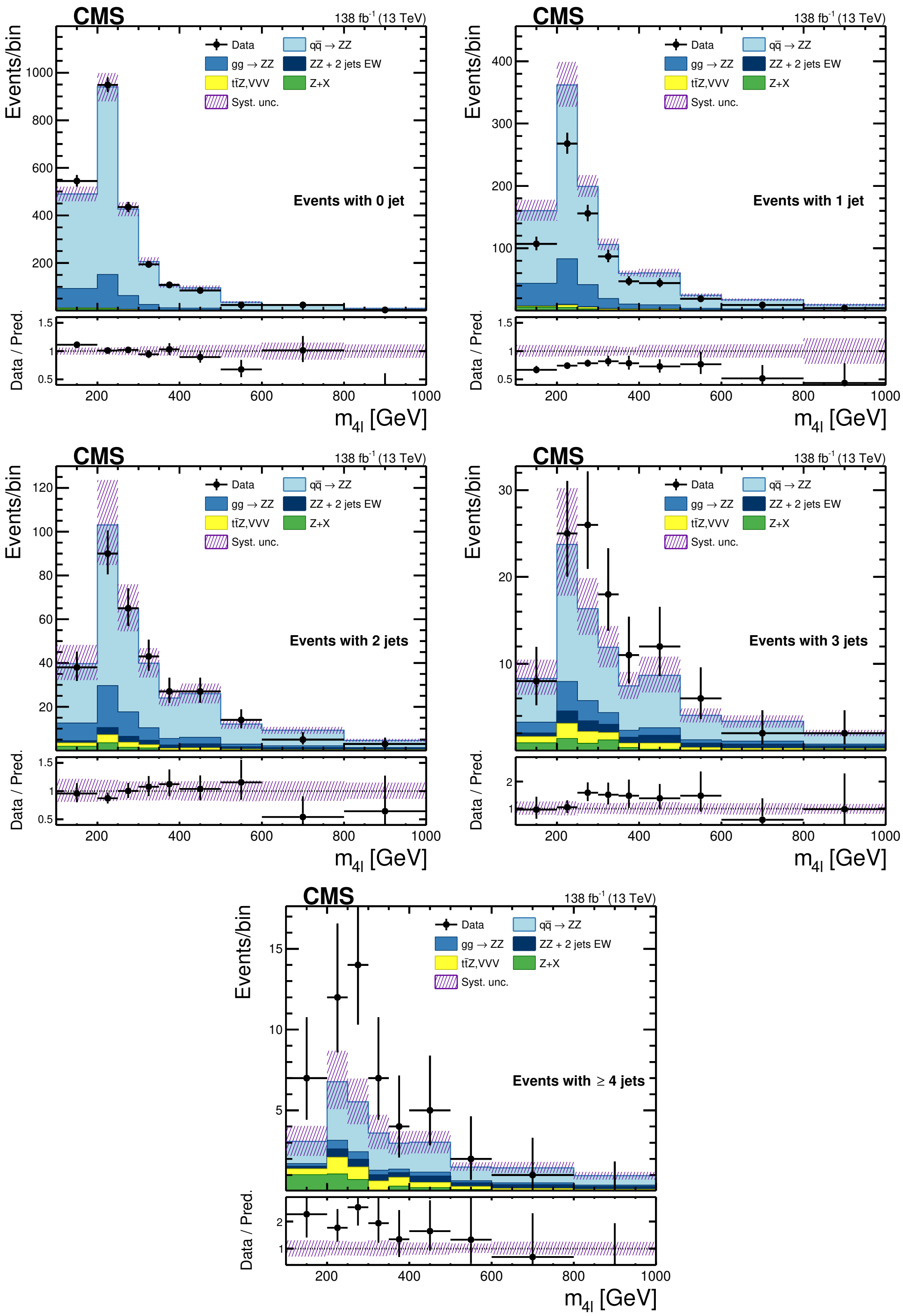

Figure 5. The $m_{4\ell}$ distributions for events with $60 < m_{Z_1,Z_2} < 120\,\text{GeV}$ and different jet multiplicities. Other details are as in the caption of figure 2.

JHEP10(2024)209

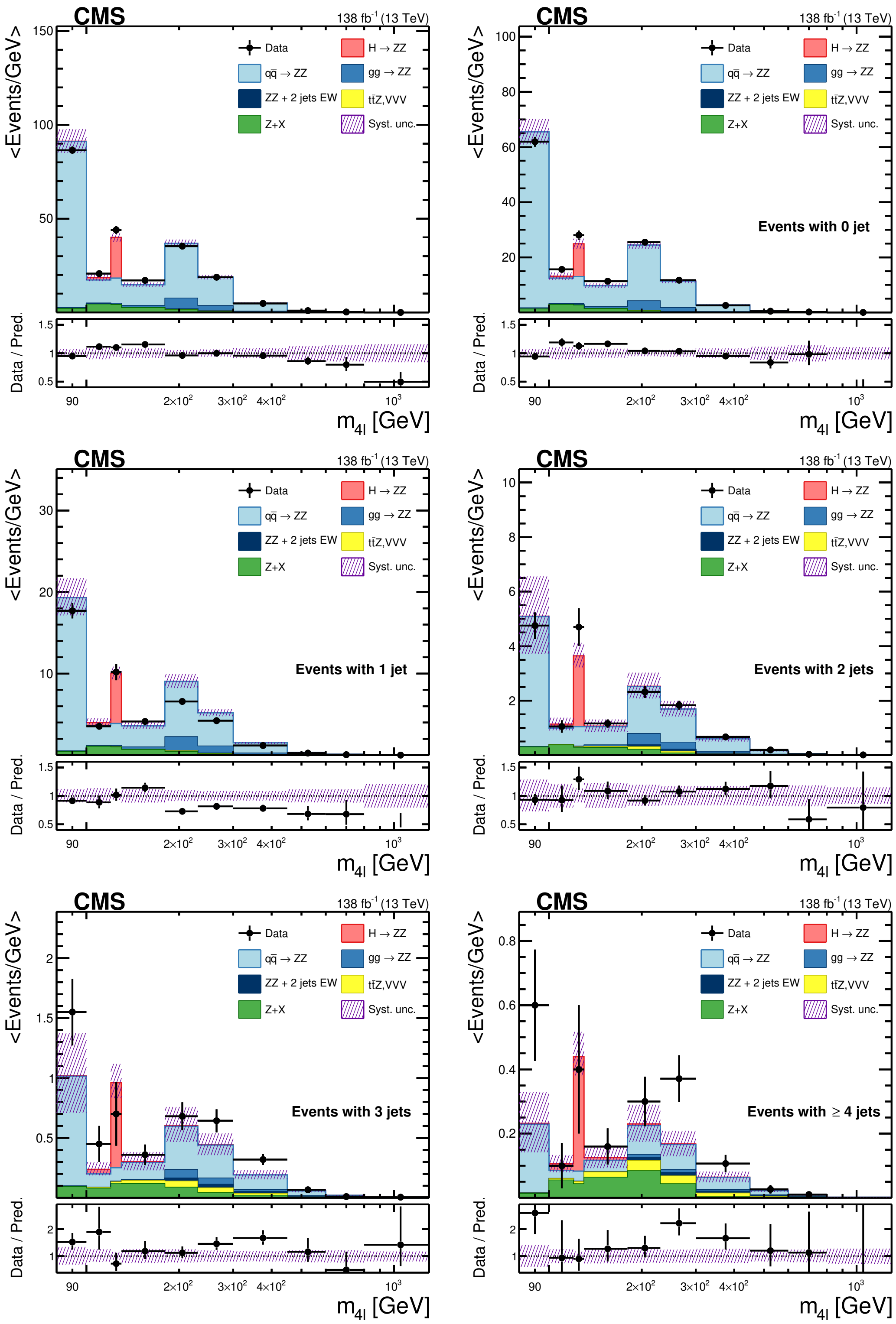

Figure 6. The $m_{4\ell}$ distributions in the full four-lepton invariant mass range for events with different jet multiplicities, normalized by bin width. Other details are as in the caption of figure 2.

JHEP10(2024)209

Process	eeee	eeμμ	μμμμ	$2\ell 2\ell'$
		$80 < m_{4\ell} < 100$ GeV		
Background	$4.6 \pm 0.5 \pm 1.8$	$15.5 \pm 1.6 \pm 6.2$	$22.8 \pm 2.1 \pm 9.1$	$43 \pm 3 \pm 17$
Signal	$216 \pm 1^{+40}_{-36}$	$731 \pm 2^{+66}_{-64}$	$841 \pm 2^{+59}_{-57}$	$1790 \pm 3^{+140}_{-140}$
Total expected	$220 \pm 1^{+40}_{-36}$	$747 \pm 3^{+66}_{-64}$	$864 \pm 3^{+59}_{-58}$	$1830 \pm 4^{+140}_{-140}$
Data	194	698	838	1730
		$60 < m_{Z_1,Z_2} < 120$ GeV		
Background	$22.9 \pm 0.9 \pm 5.7$	$46 \pm 2 \pm 10$	$28.9 \pm 1.3 \pm 6.5$	$98 \pm 2 \pm 23$
Signal	$716 \pm 2^{+63}_{-60}$	$1830 \pm 3^{+140}_{-140}$	$1138 \pm 3^{+85}_{-82}$	$3680 \pm 5^{+280}_{-270}$
Total expected	$739 \pm 2^{+63}_{-60}$	$1870 \pm 4^{+140}_{-140}$	$1167 \pm 3^{+85}_{-82}$	$3780 \pm 5^{+280}_{-270}$
Data	671	1805	1106	3582

Table 5. The observed and expected yields of ZZ events in different mass ranges, and estimated yields of background events, shown for each final state and for the sum. The first uncertainty is statistical, and the second one is systematic. (Due to rounding, the sum of individual entries may not match the total value shown.)

Process	0 jet	1 jet	2 jets	3 jets	≥4 jets
			$80 < m_{4\ell} < 100$ GeV		
Background	$25 \pm 2 \pm 10$	$9.1 \pm 1.3 \pm 3.6$	$6.1 \pm 1.0 \pm 2.4$	$1.9 \pm 0.6 \pm 0.8$	$0.4 \pm 0.3 \pm 0.1$
Signal	$1300 \pm 3^{+100}_{-100}$	$371 \pm 2^{+48}_{-45}$	$95 \pm 1^{+29}_{-28}$	$18.7 \pm 0.4^{+7.1}_{-6.2}$	$4.5 \pm 0.2^{+1.9}_{-1.8}$
Total expected	$1320 \pm 3^{+100}_{-100}$	$381 \pm 2^{+48}_{-45}$	$101 \pm 1^{+29}_{-28}$	$20.6 \pm 0.7^{+7.1}_{-6.2}$	$4.9 \pm 0.3^{+2.0}_{-1.8}$
Data	1238	354	95	31	12
			$60 < m_{Z_1,Z_2} < 120$ GeV		
Background	$29.3 \pm 1.4 \pm 8.9$	$28.6 \pm 1.2 \pm 6.7$	$21.2 \pm 0.9 \pm 3.7$	$11.6 \pm 0.7 \pm 2.0$	$7.6 \pm 0.5 \pm 1.5$
Signal	$2320 \pm 3^{+160}_{-170}$	$960 \pm 3^{+100}_{-90}$	$303 \pm 1^{+60}_{-56}$	$75 \pm 1^{+20}_{-19}$	$21.9 \pm 0.3^{+7.9}_{-7.2}$
Total expected	$2350 \pm 4^{+160}_{-170}$	$990 \pm 3^{+100}_{-100}$	$324 \pm 2^{+60}_{-56}$	$87 \pm 1^{+21}_{-19}$	$29.5 \pm 0.7^{+8.1}_{-7.4}$
Data	2367	741	312	110	52

Table 6. The observed and expected yields of ZZ events in different mass ranges, and estimated yields of background events, shown for each jet multiplicity. The first uncertainty is statistical, and the second one is systematic. (Due to rounding, the sum of individual entries may not match the total value shown.)

8.2 Differential cross sections

The unfolded differential distributions normalized to the ZZ fiducial cross section are presented in figures 7–10. Figure 7 (left) shows the normalized $d\sigma/dm_{4\ell}$ cross section. The MadGraph5_aMC@NLO, POWHEG and nNNLO+PS predictions demonstrate similar behavior and describe well the differential behavior at low $m_{4\ell}$, whereas they overestimate the measured values in the moderate to high $m_{4\ell}$ regions. This discrepancy can be mitigated with EW corrections as discussed in ref. [22]. To estimate the effect of the corrections, a differential K factor from [22] for the NLO EW corrections was applied to the nNNLO+PS predictions as a function of $m_{4\ell}$. The EW-corrected nNNLO+PS predictions describe the measured values better than those without the corrections, although at high values of $m_{4\ell}$ only within large statistical uncertainties of the measurements. The EW corrections are only significant in $m_{4\ell}$ and have negligible effect on any other normalized distribution presented in this paper; therefore in all other non-$m_{4\ell}$ distributions only nominal nNNLO+PS predictions are shown. For the $m_{4\ell}$ distributions for various jet multiplicities the EW corrections are not available and therefore these distributions do not contain EW corrections.

Figure 7 (right) shows the differential cross sections as a function of the number of jets in the events. The MadGraph5_aMC@NLO and POWHEG predictions show similar distributions. Similar to the discussion in the previous section, neither of the two MC simulations describes the 1-jet cross section, and both simulations predict too low cross sections for high jet multiplicities. On the other hand, the nNNLO+PS prediction describes the high jet multiplicity bin better than the other two predictions, whereas the agreement in the 1-jet bin is also improved. In general, the nNNLO+PS prediction describes the N_{jets} distribution better than MadGraph5_aMC@NLO and POWHEG.

Figure 8 shows the differential cross sections in bins of p_T and $|\eta|$ for the highest- and the second highest-p_T jet in events with at least one and two jets. The p_T distributions show moderate differences between data and predictions, whereas the $|\eta|$ distributions are well described within uncertainties.

Figure 9 shows the differential cross sections for dijet events as a function of (left) $|\Delta\eta|$ and (right) the dijet mass between two highest-p_T jets. Within uncertainties the dijet mass is described by the predictions, whereas $|\Delta\eta|$ measurements show a small trend with respect to the predictions.

Finally, the $\mathrm{d}\sigma/\mathrm{d}m_{4\ell}$ differential cross section is presented in figure 10 for the full four-lepton invariant mass range and inclusive in jet multiplicity. The measured normalized differential cross section is well described by the predictions. Additional $\mathrm{d}\sigma/\mathrm{d}m_{4\ell}$ differential cross sections with different jet multiplicities for the on-shell Z bosons and for the full four-lepton invariant mass range are presented in figures 11 and 12. The comparison with the theoretical predictions shows the same behavior than for the measurements presented in the previous section.

9 Summary

The four-lepton production in association with jets, $\mathrm{pp} \to (\mathrm{Z}/\gamma^*)(\mathrm{Z}/\gamma^*) + \text{jets} \to 2\ell 2\ell' + \text{jets}$, where $\ell, \ell' = \mathrm{e}$ or μ, was studied in proton-proton collisions at a center-of-mass energy of 13 TeV. The data sample corresponds to an integrated luminosity of $138\,\mathrm{fb}^{-1}$ collected with the CMS detector at the LHC during 2016–2018. Differential distributions and differential cross sections normalized to the ZZ fiducial cross section were measured with respect to various kinematic variables: number of jets, jet transverse momentum (p_T) and pseudorapidity (η), invariant mass of the dijet system and η difference between the highest-p_T and second-highest-p_T jets, and invariant mass of the four leptons ($m_{4\ell}$) for different jet multiplicities. Tabulated results are provided in HEPData [60]. In general, predictions of theoretical models agree with the data, but in some regions significant discrepancies between predicted and measured values were observed. The recent nNNLO+PS prediction improves the data/prediction agreement in the 1-jet and high jet multiplicity regions, and describes the distribution of jet multiplicities better than NLO samples generated with the event generators MadGraph5_aMC@NLO and POWHEG. The inclusion of electroweak corrections improves the description of the $m_{4\ell}$ distribution. These measurements demonstrate the necessity for better Monte Carlo modeling

JHEP10(2024)209

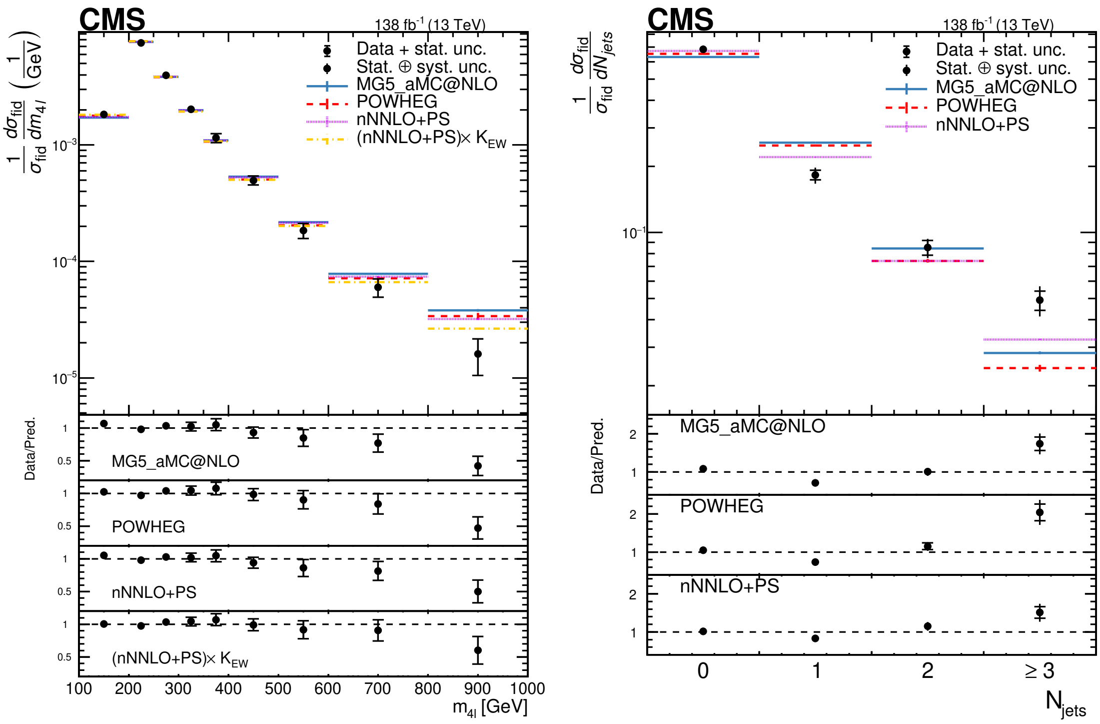

Figure 7. Differential cross sections normalized to the fiducial cross section as a function of (left) $m_{4\ell}$, (right) the number of jets with $p_{\mathrm{T}} > 30\,\mathrm{GeV}$. The on-shell Z requirement $60 < m_{\mathrm{Z}_1,\mathrm{Z}_2} < 120\,\mathrm{GeV}$ is applied. Points represent the unfolded data, solid histograms the MadGraph5_aMC@NLO $\mathrm{q\bar{q}} \to \mathrm{ZZ}$ predictions, and red dashed histograms the POWHEG $\mathrm{q\bar{q}} \to \mathrm{ZZ}$ predictions. MCFM $\mathrm{gg} \to \mathrm{ZZ}$, POWHEG $\mathrm{H} \to \mathrm{ZZ}$, and MadGraph5_aMC@NLO EW ZZ predictions are included in these two sets of predictions. The purple dashed histograms represent the nNNLO+PS predictions, and the yellow dashed histogram represents the nNNLO+PS prediction with EW corrections applied. Vertical bars on both MC predictions represent the statistical uncertainties. The lower panels show the ratio of the measured to the predicted cross sections. The vertical bars on data points with horizontal lines at the ends represent the statistical uncertainties only, whereas the vertical bars without horizontal lines at the ends represent the total uncertainties calculated as the sum in quadrature of the statistical and systematic uncertainties. The overflow is included in the last bin of the distributions.

in events with complex multiboson final states and extra jets. Further improvement of the predictions is required to describe the ZZ+jets production in the whole phase space.

Acknowledgments

We congratulate our colleagues in the CERN accelerator departments for the excellent performance of the LHC and thank the technical and administrative staffs at CERN and at other CMS institutes for their contributions to the success of the CMS effort. In addition, we gratefully acknowledge the computing centers and personnel of the Worldwide LHC Computing Grid and other centers for delivering so effectively the computing infrastructure essential to our analyses. Finally, we acknowledge the enduring support for the construction and operation of the LHC, the CMS detector, and the supporting computing infrastructure provided by the following funding agencies: SC (Armenia), BMBWF and FWF (Austria);

JHEP10(2024)209

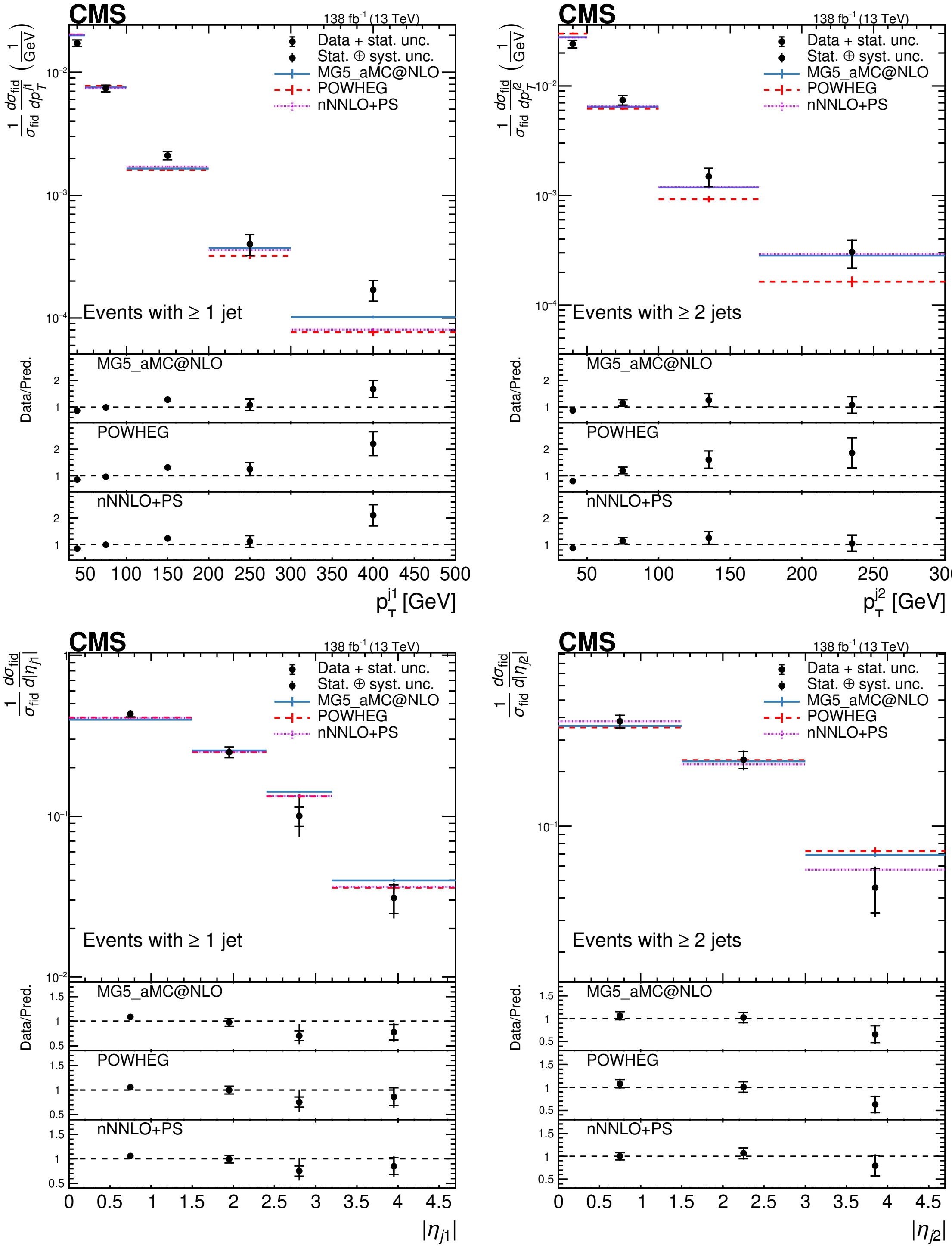

Figure 8. Differential cross sections normalized to the fiducial cross section as a function of p_T and $|\eta|$ of the highest- and the second-highest-p_T jet in events containing at least one or two jets, respectively. The on-shell Z requirement $60 < m_{Z_1,Z_2} < 120\,\mathrm{GeV}$ is applied. Other details are as in the caption of figure 7.

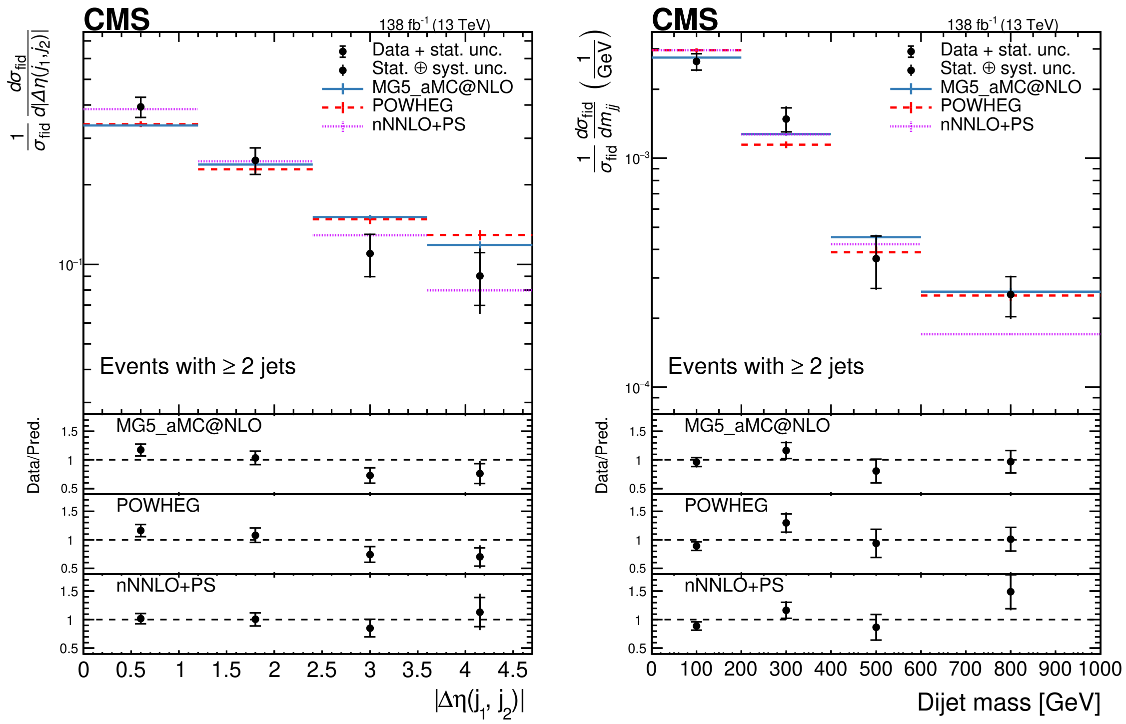

Figure 9. Differential cross sections normalized to the fiducial cross section as a function of (left) $|\Delta\eta|$ and (right) dijet mass between highest-p_T jets in events with at least two jets. Events with $60 < m_{Z_1,Z_2} < 120$ GeV requirement. Other details are as in the caption of figure 7.

FNRS and FWO (Belgium); CNPq, CAPES, FAPERJ, FAPERGS, and FAPESP (Brazil); MES and BNSF (Bulgaria); CERN; CAS, MoST, and NSFC (China); MINCIENCIAS (Colombia); MSES and CSF (Croatia); RIF (Cyprus); SENESCYT (Ecuador); ERC PRG, RVTT3 and MoER TK202 (Estonia); Academy of Finland, MEC, and HIP (Finland); CEA and CNRS/IN2P3 (France); SRNSF (Georgia); BMBF, DFG, and HGF (Germany); GSRI (Greece); NKFIH (Hungary); DAE and DST (India); IPM (Iran); SFI (Ireland); INFN (Italy); MSIP and NRF (Republic of Korea); MES (Latvia); LMTLT (Lithuania); MOE and UM (Malaysia); BUAP, CINVESTAV, CONACYT, LNS, SEP, and UASLP-FAI (Mexico); MOS (Montenegro); MBIE (New Zealand); PAEC (Pakistan); MES and NSC (Poland); FCT (Portugal); MESTD (Serbia); MCIN/AEI and PCTI (Spain); MOSTR (Sri Lanka); Swiss Funding Agencies (Switzerland); MST (Taipei); MHESI and NSTDA (Thailand); TUBITAK and TENMAK (Turkey); NASU (Ukraine); STFC (United Kingdom); DOE and NSF (U.S.A.).

Individuals have received support from the Marie-Curie program and the European Research Council and Horizon 2020 Grant, contract Nos. 675440, 724704, 752730, 758316, 765710, 824093, 101115353,101002207, and COST Action CA16108 (European Union); the Leventis Foundation; the Alfred P. Sloan Foundation; the Alexander von Humboldt Foundation; the Science Committee, project no. 22rl-037 (Armenia); the Belgian Federal Science Policy Office; the Fonds pour la Formation à la Recherche dans l'Industrie et dans l'Agriculture (FRIA-Belgium); the Agentschap voor Innovatie door Wetenschap en Technologie (IWT-Belgium); the F.R.S.-FNRS and FWO (Belgium) under the "Excellence of

JHEP10(2024)209

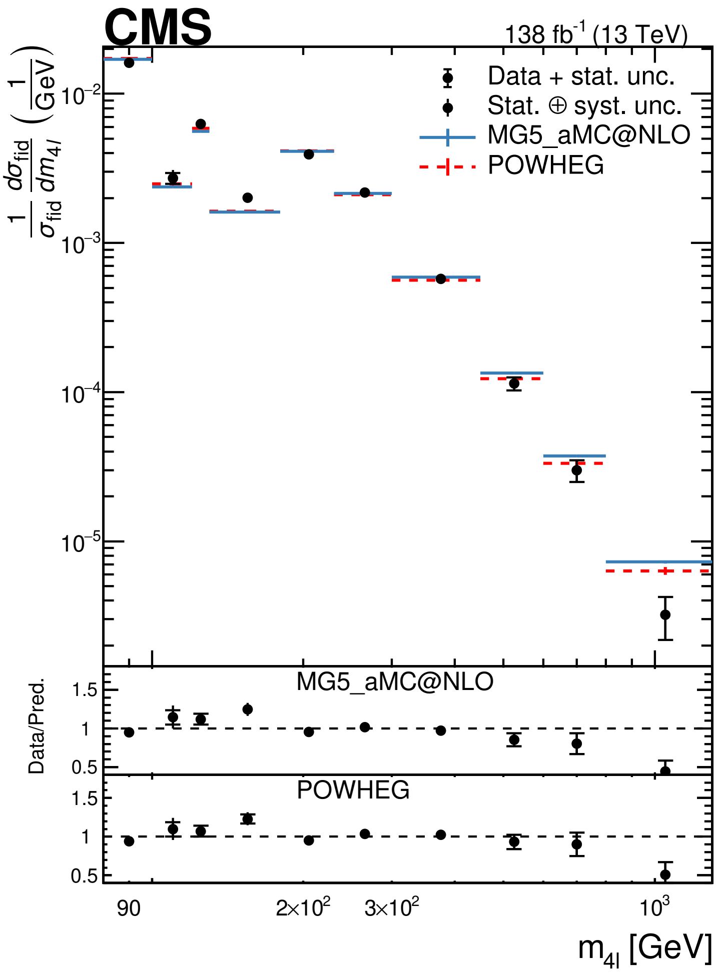

Figure 10. Differential cross sections normalized to the fiducial cross section as a function of $m_{4\ell}$ for the full four-lepton invariant mass range. Other details are as in the caption of figure 7.

Science — EOS" — be.h project n. 30820817; the Beijing Municipal Science & Technology Commission, No. Z191100007219010 and Fundamental Research Funds for the Central Universities (China); the Ministry of Education, Youth and Sports (MEYS) of the Czech Republic; the Shota Rustaveli National Science Foundation, grant FR-22-985 (Georgia); the Deutsche Forschungsgemeinschaft (DFG), under Germany's Excellence Strategy — EXC 2121 "Quantum Universe" — 390833306, and under project number 400140256 - GRK2497; the Hellenic Foundation for Research and Innovation (HFRI), Project Number 2288 (Greece); the Hungarian Academy of Sciences, the New National Excellence Program - ÚNKP, the NKFIH research grants K 131991, K 133046, K 138136, K 143460, K 143477, K 146913, K 146914, K 147048, 2020-2.2.1-ED-2021-00181, and TKP2021-NKTA-64 (Hungary); the Council of Science and Industrial Research, India; ICSC — National Research Center for High Performance Computing, Big Data and Quantum Computing, funded by the EU Nex-Generation program (Italy); the Latvian Council of Science; the Ministry of Education and Science, project no. 2022/WK/14, and the National Science Center, contracts Opus 2021/41/B/ST2/01369 and 2021/43/B/ST2/01552 (Poland); the Fundação para a Ciência

JHEP10(2024)209

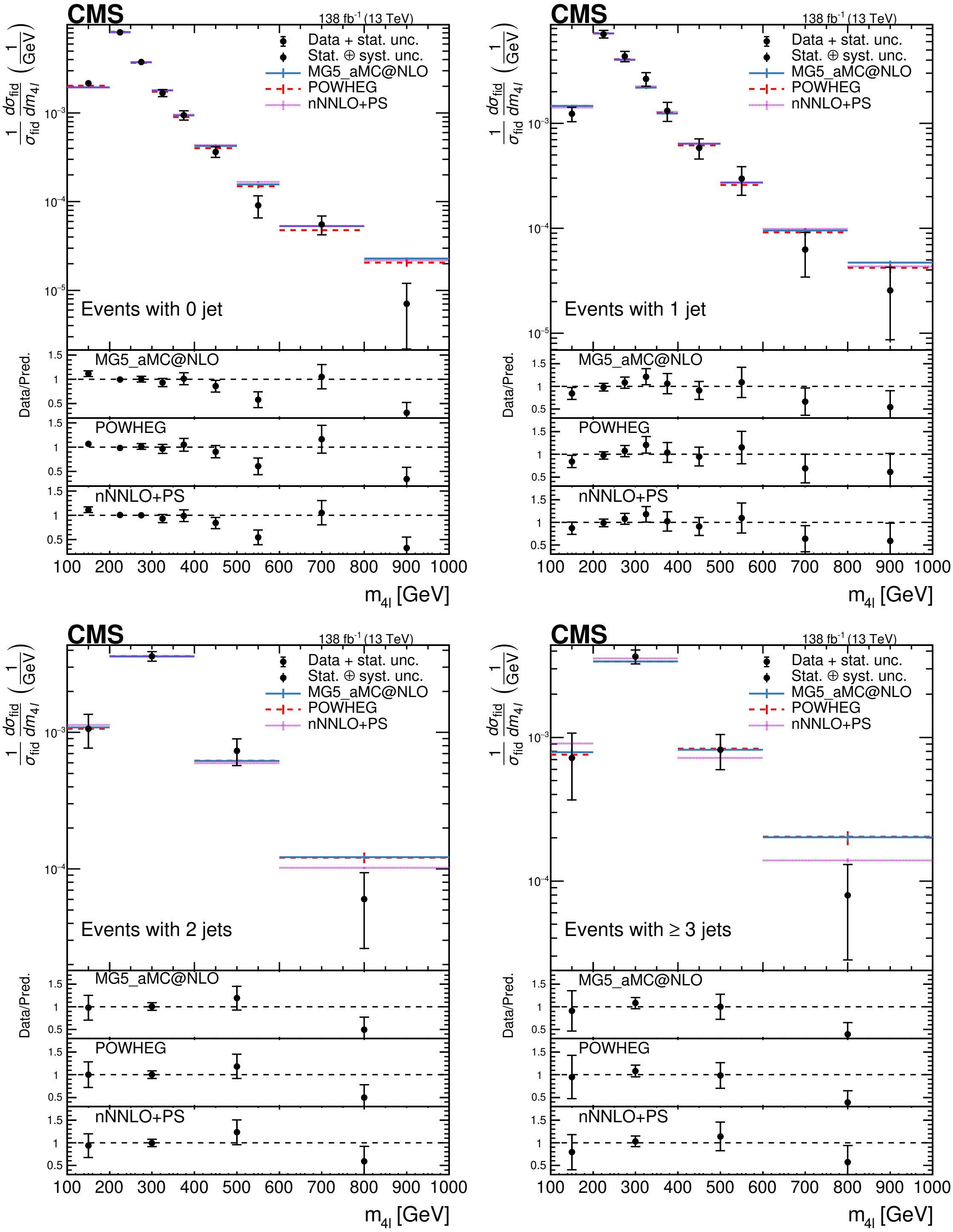

Figure 11. Differential cross sections normalized to the fiducial cross section as a function of $m_{4\ell}$ for $60 < m_{Z_1,Z_2} < 120\,\text{GeV}$ and for different jet multiplicities. Other details are as in the figure 7 caption.

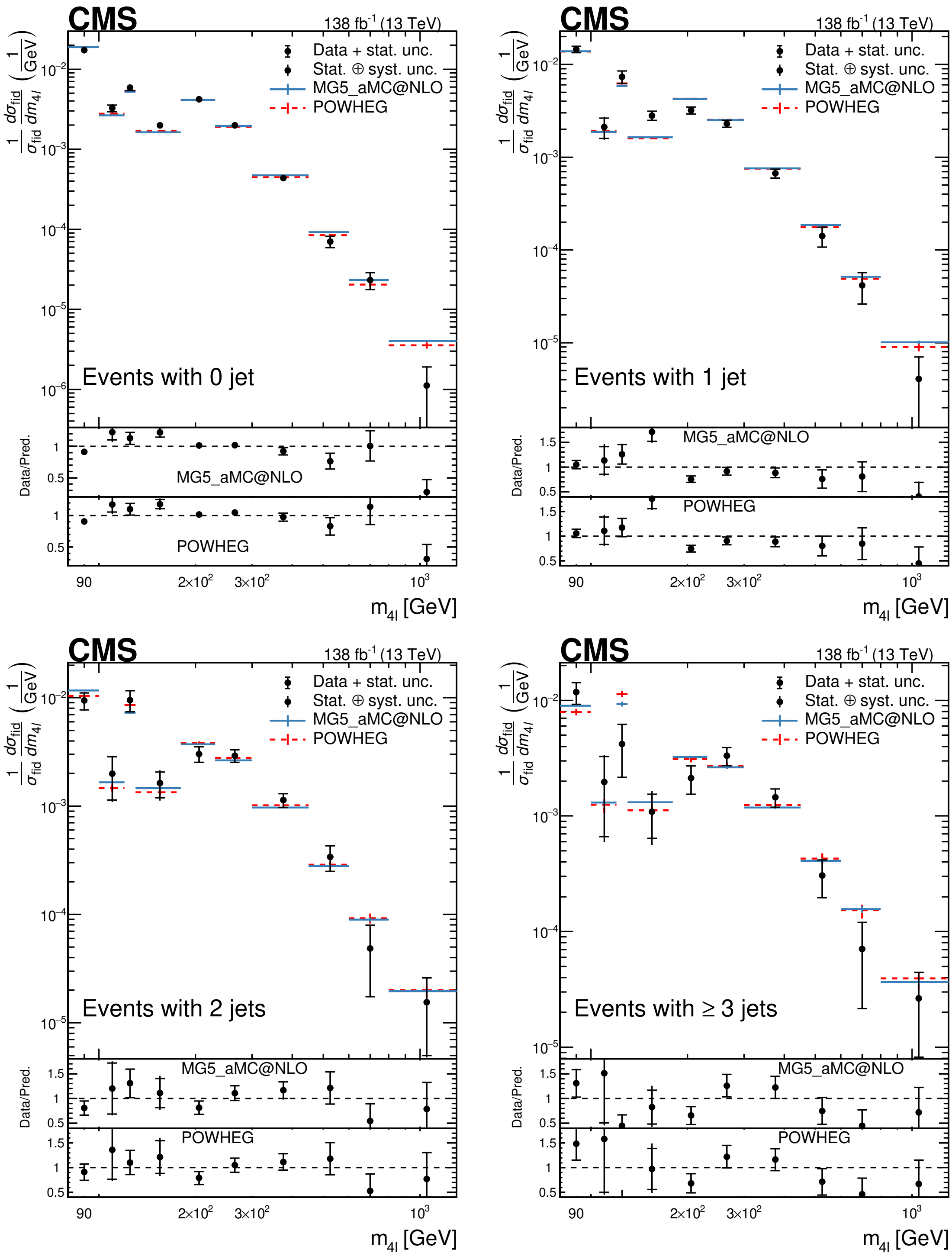

Figure 12. Differential cross sections normalized to the fiducial cross section as a function of $m_{4\ell}$ for the full four-lepton invariant mass range and different jet multiplicities. Other details are as in the figure 7 caption.

e a Tecnologia, grant CEECIND/01334/2018 (Portugal); the National Priorities Research Program by Qatar National Research Fund; MCIN/AEI/10.13039/501100011033, ERDF "a way of making Europe", and the Programa Estatal de Fomento de la Investigación Científica y Técnica de Excelencia María de Maeztu, grant MDM-2017-0765 and Programa Severo Ochoa del Principado de Asturias (Spain); the Chulalongkorn Academic into Its 2nd Century Project Advancement Project, and the National Science, Research and Innovation Fund via the Program Management Unit for Human Resources & Institutional Development, Research and Innovation, grant B37G660013 (Thailand); the Kavli Foundation; the Nvidia Corporation; the SuperMicro Corporation; the Welch Foundation, contract C-1845; and the Weston Havens Foundation (U.S.A.).

References

[1] CMS collaboration, *Measurement of the ZZ production cross section and search for anomalous couplings in $2\ell 2\ell'$ final states in pp collisions at $\sqrt{s} = 7$ TeV*, JHEP **01** (2013) 063 [arXiv:1211.4890] [INSPIRE].

[2] CMS collaboration, *Measurement of the $pp \to ZZ$ production cross section and constraints on anomalous triple gauge couplings in four-lepton final states at $\sqrt{s} = 8$ TeV*, Phys. Lett. B **740** (2015) 250 [arXiv:1406.0113] [INSPIRE].

[3] CMS collaboration, *Measurements of the ZZ production cross sections in the $2\ell 2\nu$ channel in proton-proton collisions at $\sqrt{s} = 7$ and 8 TeV and combined constraints on triple gauge couplings*, Eur. Phys. J. C **75** (2015) 511 [arXiv:1503.05467] [INSPIRE].

[4] CMS collaboration, *Measurement of the ZZ production cross section and $Z \to \ell^+\ell^-\ell'^+\ell'^-$ branching fraction in pp collisions at $\sqrt{s} = 13$ TeV*, Phys. Lett. B **763** (2016) 280 [arXiv:1607.08834] [INSPIRE].

[5] CMS collaboration, *Measurements of the $pp \to ZZ$ production cross section and the $Z \to 4\ell$ branching fraction, and constraints on anomalous triple gauge couplings at $\sqrt{s} = 13$ TeV*, Eur. Phys. J. C **78** (2018) 165 [*Erratum ibid.* **78** (2018) 515] [arXiv:1709.08601] [INSPIRE].

[6] CMS collaboration, *Measurements of the electroweak diboson production cross sections in proton-proton collisions at $\sqrt{s} = 5.02$ TeV using leptonic decays*, Phys. Rev. Lett. **127** (2021) 191801 [arXiv:2107.01137] [INSPIRE].

[7] CMS collaboration, *Measurement of differential cross sections for Z boson pair production in association with jets at $\sqrt{s} = 8$ and 13 TeV*, Phys. Lett. B **789** (2019) 19 [arXiv:1806.11073] [INSPIRE].

[8] CMS collaboration, *Measurements of $pp \to ZZ$ production cross sections and constraints on anomalous triple gauge couplings at $\sqrt{s} = 13$ TeV*, Eur. Phys. J. C **81** (2021) 200 [arXiv:2009.01186] [INSPIRE].

[9] CMS collaboration, *Evidence for electroweak production of four charged leptons and two jets in proton-proton collisions at $\sqrt{s} = 13$ TeV*, Phys. Lett. B **812** (2021) 135992 [arXiv:2008.07013] [INSPIRE].

[10] ATLAS collaboration, *Measurement of ZZ production in pp collisions at $\sqrt{s} = 7$ TeV and limits on anomalous ZZZ and $ZZ\gamma$ couplings with the ATLAS detector*, JHEP **03** (2013) 128 [arXiv:1211.6096] [INSPIRE].

[11] ATLAS collaboration, *Measurements of four-lepton production in pp collisions at $\sqrt{s} = 8$ TeV with the ATLAS detector*, Phys. Lett. B **753** (2016) 552 [arXiv:1509.07844] [INSPIRE].

[12] ATLAS collaboration, *Measurement of the ZZ production cross section in pp collisions at $\sqrt{s} = 13$ TeV with the ATLAS detector*, Phys. Rev. Lett. **116** (2016) 101801 [arXiv:1512.05314] [INSPIRE].

[13] ATLAS collaboration, *Measurement of the four-lepton invariant mass spectrum in 13 TeV proton-proton collisions with the ATLAS detector*, JHEP **04** (2019) 048 [arXiv:1902.05892] [INSPIRE].

[14] ATLAS collaboration, *Measurement of ZZ production in the $\ell\ell\nu\nu$ final state with the ATLAS detector in pp collisions at $\sqrt{s} = 13$ TeV*, JHEP **10** (2019) 127 [arXiv:1905.07163] [INSPIRE].

[15] ATLAS collaboration, *$ZZ \to \ell^+\ell^-\ell'^+\ell'^-$ cross-section measurements and search for anomalous triple gauge couplings in 13 TeV pp collisions with the ATLAS detector*, Phys. Rev. D **97** (2018) 032005 [arXiv:1709.07703] [INSPIRE].

[16] F. Cascioli et al., *ZZ production at hadron colliders in NNLO QCD*, Phys. Lett. B **735** (2014) 311 [arXiv:1405.2219] [INSPIRE].

[17] J. Alwall et al., *The automated computation of tree-level and next-to-leading order differential cross sections, and their matching to parton shower simulations*, JHEP **07** (2014) 079 [arXiv:1405.0301] [INSPIRE].

[18] S. Alioli, P. Nason, C. Oleari and E. Re, *A general framework for implementing NLO calculations in shower Monte Carlo programs: the POWHEG BOX*, JHEP **06** (2010) 043 [arXiv:1002.2581] [INSPIRE].

[19] S. Alioli, P. Nason, C. Oleari and E. Re, *NLO vector-boson production matched with shower in POWHEG*, JHEP **07** (2008) 060 [arXiv:0805.4802] [INSPIRE].

[20] P. Nason, *A new method for combining NLO QCD with shower Monte Carlo algorithms*, JHEP **11** (2004) 040 [hep-ph/0409146] [INSPIRE].

[21] S. Frixione, P. Nason and C. Oleari, *Matching NLO QCD computations with parton shower simulations: the POWHEG method*, JHEP **11** (2007) 070 [arXiv:0709.2092] [INSPIRE].

[22] L. Buonocore et al., *ZZ production at nNNLO+PS with MiNNLO$_{PS}$*, JHEP **01** (2022) 072 [arXiv:2108.05337] [INSPIRE].

[23] S. Alioli, S. Ferrario Ravasio, J.M. Lindert and R. Röntsch, *Four-lepton production in gluon fusion at NLO matched to parton showers*, Eur. Phys. J. C **81** (2021) 687 [arXiv:2102.07783] [INSPIRE].

[24] CMS collaboration, *The CMS experiment at the CERN LHC*, 2008 JINST **3** S08004 [INSPIRE].

[25] CMS collaboration, *Performance of electron reconstruction and selection with the CMS detector in proton-proton collisions at $\sqrt{s} = 8$ TeV*, 2015 JINST **10** P06005 [arXiv:1502.02701] [INSPIRE].

[26] CMS collaboration, *Performance of CMS muon reconstruction in pp collision events at $\sqrt{s} = 7$ TeV*, 2012 JINST **7** P10002 [arXiv:1206.4071] [INSPIRE].

[27] CMS collaboration, *Performance of the CMS muon detector and muon reconstruction with proton-proton collisions at $\sqrt{s} = 13$ TeV*, 2018 JINST **13** P06015 [arXiv:1804.04528] [INSPIRE].

[28] CMS collaboration, *Performance of the CMS level-1 trigger in proton-proton collisions at* $\sqrt{s} = 13$ *TeV*, 2020 *JINST* **15** P10017 [arXiv:2006.10165] [INSPIRE].

[29] CMS collaboration, *The CMS trigger system*, 2017 *JINST* **12** P01020 [arXiv:1609.02366] [INSPIRE].

[30] CMS collaboration, *Precision luminosity measurement in proton-proton collisions at* $\sqrt{s} = 13$ *TeV in 2015 and 2016 at CMS*, *Eur. Phys. J. C* **81** (2021) 800 [arXiv:2104.01927] [INSPIRE].

[31] CMS collaboration, *CMS luminosity measurement for the 2017 data-taking period at* $\sqrt{s} = 13$ *TeV*, CMS-PAS-LUM-17-004, CERN, Geneva, Switzerland (2018).

[32] CMS collaboration, *CMS luminosity measurement for the* 2018 *data-taking period at* $\sqrt{s} = 13$ *TeV*, CMS-PAS-LUM-18-002, CERN, Geneva, Switzerland (2019).

[33] J.M. Campbell and R.K. Ellis, *MCFM for the Tevatron and the LHC*, *Nucl. Phys. B Proc. Suppl.* **205-206** (2010) 10 [arXiv:1007.3492] [INSPIRE].

[34] F. Caola, K. Melnikov, R. Röntsch and L. Tancredi, *QCD corrections to ZZ production in gluon fusion at the LHC*, *Phys. Rev. D* **92** (2015) 094028 [arXiv:1509.06734] [INSPIRE].

[35] T. Sjöstrand et al., *An introduction to PYTHIA 8.2*, *Comput. Phys. Commun.* **191** (2015) 159 [arXiv:1410.3012] [INSPIRE].

[36] CMS collaboration, *Event generator tunes obtained from underlying event and multiparton scattering measurements*, *Eur. Phys. J. C* **76** (2016) 155 [arXiv:1512.00815] [INSPIRE].

[37] CMS collaboration, *Extraction and validation of a new set of CMS PYTHIA8 tunes from underlying-event measurements*, *Eur. Phys. J. C* **80** (2020) 4 [arXiv:1903.12179] [INSPIRE].

[38] NNPDF collaboration, *Parton distributions for the LHC run II*, *JHEP* **04** (2015) 040 [arXiv:1410.8849] [INSPIRE].

[39] P.F. Monni et al., *MiNNLO$_{PS}$: a new method to match NNLO QCD to parton showers*, *JHEP* **05** (2020) 143 [*Erratum ibid.* **02** (2022) 031] [arXiv:1908.06987] [INSPIRE].

[40] R. Frederix and S. Frixione, *Merging meets matching in MC@NLO*, *JHEP* **12** (2012) 061 [arXiv:1209.6215] [INSPIRE].

[41] GEANT4 collaboration, *GEANT4 — a simulation toolkit*, *Nucl. Instrum. Meth. A* **506** (2003) 250 [INSPIRE].

[42] CMS collaboration, *Particle-flow reconstruction and global event description with the CMS detector*, 2017 *JINST* **12** P10003 [arXiv:1706.04965] [INSPIRE].

[43] D. Contardo et al., *Technical proposal for the phase-II upgrade of the CMS detector*, CERN-LHCC-2015-010, CERN, Geneva, Switzerland (2015) [DOI:10.17181/CERN.VU8I.D59J].

[44] CMS collaboration, *Measurements of production cross sections of the Higgs boson in the four-lepton final state in proton-proton collisions at* $\sqrt{s} = 13$ *TeV*, *Eur. Phys. J. C* **81** (2021) 488 [arXiv:2103.04956] [INSPIRE].

[45] CMS collaboration, *Muon identification using multivariate techniques in the CMS experiment in proton-proton collisions at* $\sqrt{s} = 13$ *TeV*, 2024 *JINST* **19** P02031 [arXiv:2310.03844] [INSPIRE].

[46] CMS collaboration, *Pileup mitigation at CMS in* 13 *TeV data*, 2020 *JINST* **15** P09018 [arXiv:2003.00503] [INSPIRE].

[47] M. Cacciari and G.P. Salam, *Pileup subtraction using jet areas*, *Phys. Lett. B* **659** (2008) 119 [arXiv:0707.1378] [INSPIRE].

[48] CMS collaboration, *Measurement of the inclusive W and Z production cross sections in pp collisions at $\sqrt{s} = 7$ TeV*, *JHEP* **10** (2011) 132 [arXiv:1107.4789] [INSPIRE].

[49] M. Cacciari, G.P. Salam and G. Soyez, *The anti-k_t jet clustering algorithm*, *JHEP* **04** (2008) 063 [arXiv:0802.1189] [INSPIRE].

[50] M. Cacciari, G.P. Salam and G. Soyez, *FastJet user manual*, *Eur. Phys. J. C* **72** (2012) 1896 [arXiv:1111.6097] [INSPIRE].

[51] CMS collaboration, *Jet algorithms performance in 13 TeV data*, CMS-PAS-JME-16-003, CERN, Geneva, Switzerland (2017).

[52] CMS collaboration, *Determination of jet energy calibration and transverse momentum resolution in CMS*, 2011 *JINST* **6** P11002 [arXiv:1107.4277] [INSPIRE].

[53] CMS collaboration, *Jet energy scale and resolution in the CMS experiment in pp collisions at 8 TeV*, 2017 *JINST* **12** P02014 [arXiv:1607.03663] [INSPIRE].

[54] Particle Data Group collaboration, *Review of particle physics*, *PTEP* **2022** (2022) 083C01 [INSPIRE].

[55] CMS collaboration, *Measurement of the properties of a Higgs boson in the four-lepton final state*, *Phys. Rev. D* **89** (2014) 092007 [arXiv:1312.5353] [INSPIRE].

[56] G. D'Agostini, *A multidimensional unfolding method based on Bayes' theorem*, *Nucl. Instrum. Meth. A* **362** (1995) 487 [INSPIRE].

[57] T. Adye, *Unfolding algorithms and tests using RooUnfold*, in the proceedings of the *PHYSTAT 2011*, CERN, Geneva, Switzerland (2011) [DOI:10.5170/CERN-2011-006.313] [arXiv:1105.1160] [INSPIRE].

[58] CMS collaboration, *Measurement of the inelastic proton-proton cross section at $\sqrt{s} = 13$ TeV*, *JHEP* **07** (2018) 161 [arXiv:1802.02613] [INSPIRE].

[59] J. Butterworth et al., *PDF4LHC recommendations for LHC run II*, *J. Phys. G* **43** (2016) 023001 [arXiv:1510.03865] [INSPIRE].

[60] *HEPData record for this analysis*, CMS-SMP-22-001, CERN, Geneva, Switzerland (2023).

The CMS collaboration

Yerevan Physics Institute, Yerevan, Armenia
A. Hayrapetyan, A. Tumasyan[1]

Institut für Hochenergiephysik, Vienna, Austria
W. Adam, J.W. Andrejkovic, T. Bergauer, S. Chatterjee, K. Damanakis, M. Dragicevic, A. Escalante Del Valle, P.S. Hussain, M. Jeitler[2], N. Krammer, D. Liko, I. Mikulec, J. Schieck[2], R. Schöfbeck, D. Schwarz, M. Sonawane, S. Templ, W. Waltenberger, C.-E. Wulz[2]

Universiteit Antwerpen, Antwerpen, Belgium
M.R. Darwish[3], T. Janssen, P. Van Mechelen

Vrije Universiteit Brussel, Brussel, Belgium
E.S. Bols, J. D'Hondt, S. Dansana, A. De Moor, M. Delcourt, H. El Faham, S. Lowette, I. Makarenko, D. Müller, A.R. Sahasransu, S. Tavernier, M. Tytgat[4], S. Van Putte, D. Vannerom

Université Libre de Bruxelles, Bruxelles, Belgium
B. Clerbaux, G. De Lentdecker, L. Favart, D. Hohov, J. Jaramillo, A. Khalilzadeh, K. Lee, M. Mahdavikhorrami, A. Malara, S. Paredes, L. Pétré, N. Postiau, L. Thomas, M. Vanden Bemden, C. Vander Velde, P. Vanlaer

Ghent University, Ghent, Belgium
M. De Coen, D. Dobur, Y. Hong, J. Knolle, L. Lambrecht, G. Mestdach, C. Rendón, A. Samalan, K. Skovpen, N. Van Den Bossche, L. Wezenbeek

Université Catholique de Louvain, Louvain-la-Neuve, Belgium
A. Benecke, G. Bruno, C. Caputo, C. Delaere, I.S. Donertas, A. Giammanco, K. Jaffel, Sa. Jain, V. Lemaitre, J. Lidrych, P. Mastrapasqua, K. Mondal, T.T. Tran, S. Wertz

Centro Brasileiro de Pesquisas Fisicas, Rio de Janeiro, Brazil
G.A. Alves, E. Coelho, C. Hensel, T. Menezes De Oliveira, A. Moraes, P. Rebello Teles, M. Soeiro

Universidade do Estado do Rio de Janeiro, Rio de Janeiro, Brazil
W.L. Aldá Júnior, M. Alves Gallo Pereira, M. Barroso Ferreira Filho, H. Brandao Malbouisson, W. Carvalho, J. Chinellato[5], E.M. Da Costa, G.G. Da Silveira[6], D. De Jesus Damiao, S. Fonseca De Souza, J. Martins[7], C. Mora Herrera, K. Mota Amarilo, L. Mundim, H. Nogima, A. Santoro, S.M. Silva Do Amaral, A. Sznajder, M. Thiel, A. Vilela Pereira

Universidade Estadual Paulista, Universidade Federal do ABC, São Paulo, Brazil
C.A. Bernardes[6], L. Calligaris, T.R. Fernandez Perez Tomei, E.M. Gregores, P.G. Mercadante, S.F. Novaes, B. Orzari, Sandra S. Padula

JHEP10(2024)209

Institute for Nuclear Research and Nuclear Energy, Bulgarian Academy of Sciences, Sofia, Bulgaria
A. Aleksandrov, G. Antchev, R. Hadjiiska, P. Iaydjiev, M. Misheva, M. Shopova, G. Sultanov

University of Sofia, Sofia, Bulgaria
A. Dimitrov, T. Ivanov, L. Litov, B. Pavlov, P. Petkov, A. Petrov, E. Shumka

Instituto De Alta Investigación, Universidad de Tarapacá, Casilla 7 D, Arica, Chile
S. Keshri, S. Thakur

Beihang University, Beijing, China
T. Cheng, Q. Guo, T. Javaid, M. Mittal, L. Yuan

Department of Physics, Tsinghua University, Beijing, China
G. Bauer[8,9], Z. Hu, J. Liu, K. Yi[8,10]

Institute of High Energy Physics, Beijing, China
G.M. Chen[11], H.S. Chen[11], M. Chen[11], F. Iemmi, C.H. Jiang, A. Kapoor[12], H. Liao, Z.-A. Liu[13], F. Monti, M.A. Shahzad[11], R. Sharma[14], J.N. Song[13], J. Tao, C. Wang[11], J. Wang, Z. Wang[11], H. Zhang

State Key Laboratory of Nuclear Physics and Technology, Peking University, Beijing, China
A. Agapitos, Y. Ban, A. Levin, C. Li, Q. Li, Y. Mao, S.J. Qian, X. Sun, D. Wang, H. Yang, L. Zhang, C. Zhou

Sun Yat-Sen University, Guangzhou, China
Z. You

University of Science and Technology of China, Hefei, China
N. Lu

Institute of Modern Physics and Key Laboratory of Nuclear Physics and Ion-beam Application (MOE) - Fudan University, Shanghai, China
X. Gao[15], D. Leggat, H. Okawa, Y. Zhang

Zhejiang University, Hangzhou, Zhejiang, China
Z. Lin, C. Lu, M. Xiao

Universidad de Los Andes, Bogota, Colombia
C. Avila, D.A. Barbosa Trujillo, A. Cabrera, C. Florez, J. Fraga, J.A. Reyes Vega

Universidad de Antioquia, Medellin, Colombia
J. Mejia Guisao, F. Ramirez, M. Rodriguez, J.D. Ruiz Alvarez

JHEP10(2024)209

University of Split, Faculty of Electrical Engineering, Mechanical Engineering and Naval Architecture, Split, Croatia
D. Giljanovic, N. Godinovic, D. Lelas, A. Sculac

University of Split, Faculty of Science, Split, Croatia
M. Kovac, T. Sculac

Institute Rudjer Boskovic, Zagreb, Croatia
P. Bargassa, V. Brigljevic, B.K. Chitroda, D. Ferencek, S. Mishra, A. Starodumov[16], T. Susa

University of Cyprus, Nicosia, Cyprus
A. Attikis, K. Christoforou, S. Konstantinou, J. Mousa, C. Nicolaou, F. Ptochos, P.A. Razis, H. Rykaczewski, H. Saka, A. Stepennov

Charles University, Prague, Czech Republic
M. Finger, M. Finger Jr., A. Kveton

Escuela Politecnica Nacional, Quito, Ecuador
E. Ayala

Universidad San Francisco de Quito, Quito, Ecuador
E. Carrera Jarrin

Academy of Scientific Research and Technology of the Arab Republic of Egypt, Egyptian Network of High Energy Physics, Cairo, Egypt
A.A. Abdelalim[17,18], E. Salama[19,20]

Center for High Energy Physics (CHEP-FU), Fayoum University, El-Fayoum, Egypt
M.A. Mahmoud, Y. Mohammed

National Institute of Chemical Physics and Biophysics, Tallinn, Estonia
R.K. Dewanjee[21], K. Ehataht, M. Kadastik, T. Lange, S. Nandan, C. Nielsen, J. Pata, M. Raidal, L. Tani, C. Veelken

Department of Physics, University of Helsinki, Helsinki, Finland
H. Kirschenmann, K. Osterberg, M. Voutilainen

Helsinki Institute of Physics, Helsinki, Finland
S. Bharthuar, E. Brücken, F. Garcia, J. Havukainen, K.T.S. Kallonen, M.S. Kim, R. Kinnunen, T. Lampén, K. Lassila-Perini, S. Lehti, T. Lindén, M. Lotti, L. Martikainen, M. Myllymäki, M.m. Rantanen, H. Siikonen, E. Tuominen, J. Tuominiemi

Lappeenranta-Lahti University of Technology, Lappeenranta, Finland
P. Luukka, H. Petrow, T. Tuuva[†]

JHEP10(2024)209

IRFU, CEA, Université Paris-Saclay, Gif-sur-Yvette, France
M. Besancon, F. Couderc, M. Dejardin, D. Denegri, J.L. Faure, F. Ferri, S. Ganjour, P. Gras, G. Hamel de Monchenault, V. Lohezic, J. Malcles, J. Rander, A. Rosowsky, M.Ö. Sahin, A. Savoy-Navarro[22], P. Simkina, M. Titov

Laboratoire Leprince-Ringuet, CNRS/IN2P3, Ecole Polytechnique, Institut Polytechnique de Paris, Palaiseau, France
C. Baldenegro Barrera, F. Beaudette, A. Buchot Perraguin, P. Busson, A. Cappati, C. Charlot, F. Damas, O. Davignon, A. De Wit, G. Falmagne, B.A. Fontana Santos Alves, S. Ghosh, A. Gilbert, R. Granier de Cassagnac, A. Hakimi, B. Harikrishnan, L. Kalipoliti, G. Liu, J. Motta, M. Nguyen, C. Ochando, L. Portales, R. Salerno, U. Sarkar, J.B. Sauvan, Y. Sirois, A. Tarabini, E. Vernazza, A. Zabi, A. Zghiche

Université de Strasbourg, CNRS, IPHC UMR 7178, Strasbourg, France
J.-L. Agram[23], J. Andrea, D. Apparu, D. Bloch, J.-M. Brom, E.C. Chabert, C. Collard, S. Falke, U. Goerlach, C. Grimault, R. Haeberle, A.-C. Le Bihan, M.A. Sessini, P. Van Hove

Institut de Physique des 2 Infinis de Lyon (IP2I), Villeurbanne, France
S. Beauceron, B. Blancon, G. Boudoul, N. Chanon, J. Choi, D. Contardo, P. Depasse, C. Dozen[24], H. El Mamouni, J. Fay, S. Gascon, M. Gouzevitch, C. Greenberg, G. Grenier, B. Ille, I.B. Laktineh, M. Lethuillier, L. Mirabito, S. Perries, A. Purohit, M. Vander Donckt, P. Verdier, J. Xiao

Georgian Technical University, Tbilisi, Georgia
I. Lomidze, T. Toriashvili[25], Z. Tsamalaidze[16]

RWTH Aachen University, I. Physikalisches Institut, Aachen, Germany
V. Botta, L. Feld, K. Klein, M. Lipinski, D. Meuser, A. Pauls, N. Röwert, M. Teroerde

RWTH Aachen University, III. Physikalisches Institut A, Aachen, Germany
S. Diekmann, A. Dodonova, N. Eich, D. Eliseev, F. Engelke, M. Erdmann, P. Fackeldey, B. Fischer, T. Hebbeker, K. Hoepfner, F. Ivone, A. Jung, M.y. Lee, L. Mastrolorenzo, M. Merschmeyer, A. Meyer, S. Mukherjee, D. Noll, A. Novak, F. Nowotny, A. Pozdnyakov, Y. Rath, W. Redjeb, F. Rehm, H. Reithler, V. Sarkisovi, A. Schmidt, S.C. Schuler, A. Sharma, A. Stein, F. Torres Da Silva De Araujo[26], L. Vigilante, S. Wiedenbeck, S. Zaleski

RWTH Aachen University, III. Physikalisches Institut B, Aachen, Germany
C. Dziwok, G. Flügge, W. Haj Ahmad[27], T. Kress, A. Nowack, O. Pooth, A. Stahl, T. Ziemons, A. Zotz

Deutsches Elektronen-Synchrotron, Hamburg, Germany
H. Aarup Petersen, M. Aldaya Martin, J. Alimena, S. Amoroso, Y. An, S. Baxter, M. Bayatmakou, H. Becerril Gonzalez, O. Behnke, A. Belvedere, S. Bhattacharya,

F. Blekman[28], K. Borras[29], D. Brunner, A. Campbell, A. Cardini, C. Cheng, F. Colombina, S. Consuegra Rodríguez, G. Correia Silva, M. De Silva, G. Eckerlin, D. Eckstein, L.I. Estevez Banos, O. Filatov, E. Gallo[28], A. Geiser, A. Giraldi, G. Greau, V. Guglielmi, M. Guthoff, A. Hinzmann, A. Jafari[30], L. Jeppe, N.Z. Jomhari, B. Kaech, M. Kasemann, H. Kaveh, C. Kleinwort, R. Kogler, M. Komm, D. Krücker, W. Lange, D. Leyva Pernia, K. Lipka[31], W. Lohmann[32], R. Mankel, I.-A. Melzer-Pellmann, M. Mendizabal Morentin, J. Metwally, A.B. Meyer, G. Milella, A. Mussgiller, A. Nürnberg, Y. Otarid, D. Pérez Adán, E. Ranken, A. Raspereza, B. Ribeiro Lopes, J. Rübenach, A. Saggio, M. Scham[33,29], S. Schnake[29], P. Schütze, C. Schwanenberger[28], D. Selivanova, M. Shchedrolosiev, R.E. Sosa Ricardo, L.P. Sreelatha Pramod, D. Stafford, F. Vazzoler, A. Ventura Barroso, R. Walsh, Q. Wang, Y. Wen, K. Wichmann, L. Wiens[29], C. Wissing, S. Wuchterl, Y. Yang, A. Zimermmane Castro Santos

University of Hamburg, Hamburg, Germany

A. Albrecht, S. Albrecht, M. Antonello, S. Bein, L. Benato, M. Bonanomi, P. Connor, M. Eich, K. El Morabit, Y. Fischer, A. Fröhlich, C. Garbers, E. Garutti, A. Grohsjean, M. Hajheidari, J. Haller, H.R. Jabusch, G. Kasieczka, P. Keicher, R. Klanner, W. Korcari, T. Kramer, V. Kutzner, F. Labe, J. Lange, A. Lobanov, C. Matthies, A. Mehta, L. Moureaux, M. Mrowietz, A. Nigamova, Y. Nissan, A. Paasch, K.J. Pena Rodriguez, T. Quadfasel, B. Raciti, M. Rieger, D. Savoiu, J. Schindler, P. Schleper, M. Schröder, J. Schwandt, M. Sommerhalder, H. Stadie, G. Steinbrück, A. Tews, M. Wolf

Karlsruher Institut fuer Technologie, Karlsruhe, Germany

S. Brommer, M. Burkart, E. Butz, T. Chwalek, A. Dierlamm, A. Droll, N. Faltermann, M. Giffels, A. Gottmann, F. Hartmann[34], R. Hofsaess, M. Horzela, U. Husemann, M. Klute, R. Koppenhöfer, M. Link, A. Lintuluoto, S. Maier, S. Mitra, M. Mormile, Th. Müller, M. Neukum, M. Oh, G. Quast, K. Rabbertz, B. Regnery, N. Shadskiy, I. Shvetsov, H.J. Simonis, N. Trevisani, R. Ulrich, J. van der Linden, R.F. Von Cube, M. Wassmer, S. Wieland, F. Wittig, R. Wolf, S. Wunsch, X. Zuo

Institute of Nuclear and Particle Physics (INPP), NCSR Demokritos, Aghia Paraskevi, Greece

G. Anagnostou, P. Assiouras, G. Daskalakis, A. Kyriakis, A. Papadopoulos[34], A. Stakia

National and Kapodistrian University of Athens, Athens, Greece

P. Kontaxakis, G. Melachroinos, A. Panagiotou, I. Papavergou, I. Paraskevas, N. Saoulidou, K. Theofilatos, E. Tziaferi, K. Vellidis, I. Zisopoulos

National Technical University of Athens, Athens, Greece

G. Bakas, T. Chatzistavrou, G. Karapostoli, K. Kousouris, I. Papakrivopoulos, E. Siamarkou, G. Tsipolitis, A. Zacharopoulou

University of Ioánnina, Ioánnina, Greece

K. Adamidis, I. Bestintzanos, I. Evangelou, C. Foudas, P. Gianneios, C. Kamtsikis, P. Katsoulis, P. Kokkas, P.G. Kosmoglou Kioseoglou, N. Manthos, I. Papadopoulos, J. Strologas

JHEP10(2024)209

HUN-REN Wigner Research Centre for Physics, Budapest, Hungary
M. Bartók[35], C. Hajdu, D. Horvath[36,37], F. Sikler, V. Veszpremi

MTA-ELTE Lendület CMS Particle and Nuclear Physics Group, Eötvös Loránd University, Budapest, Hungary
M. Csanád, K. Farkas, M.M.A. Gadallah[38], Á. Kadlecsik, P. Major, K. Mandal, G. Pásztor, A.J. Rádl[39], G.I. Veres

Faculty of Informatics, University of Debrecen, Debrecen, Hungary
P. Raics, B. Ujvari[40], G. Zilizi

Institute of Nuclear Research ATOMKI, Debrecen, Hungary
G. Bencze, S. Czellar, J. Karancsi[35], J. Molnar, Z. Szillasi

Karoly Robert Campus, MATE Institute of Technology, Gyongyos, Hungary
T. Csorgo[39], F. Nemes[39], T. Novak

Panjab University, Chandigarh, India
J. Babbar, S. Bansal, S.B. Beri, V. Bhatnagar, G. Chaudhary, S. Chauhan, N. Dhingra[41], R. Gupta, A. Kaur, A. Kaur, H. Kaur, M. Kaur, S. Kumar, M. Meena, K. Sandeep, T. Sheokand, J.B. Singh, A. Singla

University of Delhi, Delhi, India
A. Ahmed, A. Bhardwaj, A. Chhetri, B.C. Choudhary, A. Kumar, M. Naimuddin, K. Ranjan, S. Saumya

Saha Institute of Nuclear Physics, HBNI, Kolkata, India
S. Acharya[42], S. Baradia, S. Barman[43], S. Bhattacharya, D. Bhowmik, S. Dutta, S. Dutta, B. Gomber[42], P. Palit, G. Saha, B. Sahu[42], S. Sarkar

Indian Institute of Technology Madras, Madras, India
M.M. Ameen, P.K. Behera, S.C. Behera, S. Chatterjee, P. Jana, P. Kalbhor, J.R. Komaragiri[44], D. Kumar[44], L. Panwar[44], R. Pradhan, P.R. Pujahari, N.R. Saha, A. Sharma, A.K. Sikdar, S. Verma

Tata Institute of Fundamental Research-A, Mumbai, India
T. Aziz, I. Das, S. Dugad, M. Kumar, G.B. Mohanty, P. Suryadevara

Tata Institute of Fundamental Research-B, Mumbai, India
A. Bala, S. Banerjee, R.M. Chatterjee, M. Guchait, Sh. Jain, S. Karmakar, S. Kumar, G. Majumder, K. Mazumdar, S. Mukherjee, S. Parolia, A. Thachayath

National Institute of Science Education and Research, An OCC of Homi Bhabha National Institute, Bhubaneswar, Odisha, India
S. Bahinipati[45], A.K. Das, C. Kar, D. Maity[46], P. Mal, T. Mishra, V.K. Muraleedharan Nair Bindhu[46], K. Naskar[46], A. Nayak[46], P. Sadangi, P. Saha, S.K. Swain, S. Varghese[46], D. Vats[46]

JHEP10(2024)209

Indian Institute of Science Education and Research (IISER), Pune, India
A. Alpana, S. Dube, B. Kansal, A. Laha, A. Rastogi, S. Sharma

Isfahan University of Technology, Isfahan, Iran
H. Bakhshiansohi[47], E. Khazaie[48], M. Zeinali[49]

Institute for Research in Fundamental Sciences (IPM), Tehran, Iran
S. Chenarani[50], S.M. Etesami, M. Khakzad, M. Mohammadi Najafabadi

University College Dublin, Dublin, Ireland
M. Grunewald

INFN Sezione di Bari[a], Università di Bari[b], Politecnico di Bari[c], Bari, Italy
M. Abbrescia[a,b], R. Aly[a,c,17], A. Colaleo[a,b], D. Creanza[a,c], B. D'Anzi[a,b], N. De Filippis[a,c], M. De Palma[a,b], A. Di Florio[a,c], W. Elmetenawee[a,b,17], L. Fiore[a], G. Iaselli[a,c], G. Maggi[a,c], M. Maggi[a], I. Margjeka[a,b], V. Mastrapasqua[a,b], S. My[a,b], S. Nuzzo[a,b], A. Pellecchia[a,b], A. Pompili[a,b], G. Pugliese[a,c], R. Radogna[a], G. Ramirez-Sanchez[a,c], D. Ramos[a], A. Ranieri[a], L. Silvestris[a], F.M. Simone[a,b], Ü. Sözbilir[a], A. Stamerra[a], R. Venditti[a], P. Verwilligen[a], A. Zaza[a,b]

INFN Sezione di Bologna[a], Università di Bologna[b], Bologna, Italy
G. Abbiendi[a], C. Battilana[a,b], D. Bonacorsi[a,b], L. Borgonovi[a], R. Campanini[a,b], P. Capiluppi[a,b], A. Castro[a,b], M. Cuffiani[a,b], G.M. Dallavalle[a], T. Diotalevi[a,b], F. Fabbri[a], A. Fanfani[a,b], D. Fasanella[a,b], P. Giacomelli[a], L. Giommi[a,b], C. Grandi[a], L. Guiducci[a,b], S. Lo Meo[a,51], L. Lunerti[a,b], S. Marcellini[a], G. Masetti[a], F.L. Navarria[a,b], A. Perrotta[a], F. Primavera[a,b], A.M. Rossi[a,b], T. Rovelli[a,b], G.P. Siroli[a,b]

INFN Sezione di Catania[a], Università di Catania[b], Catania, Italy
S. Costa[a,b,52], A. Di Mattia[a], R. Potenza[a,b], A. Tricomi[a,b,52], C. Tuve[a,b]

INFN Sezione di Firenze[a], Università di Firenze[b], Firenze, Italy
G. Barbagli[a], G. Bardelli[a,b], B. Camaiani[a,b], A. Cassese[a], R. Ceccarelli[a], V. Ciulli[a,b], C. Civinini[a], R. D'Alessandro[a,b], E. Focardi[a,b], T. Kello[a], G. Latino[a,b], P. Lenzi[a,b], M. Lizzo[a], M. Meschini[a], S. Paoletti[a], A. Papanastassiou[a,b], G. Sguazzoni[a], L. Viliani[a]

INFN Laboratori Nazionali di Frascati, Frascati, Italy
L. Benussi, S. Bianco, S. Meola[53], D. Piccolo

INFN Sezione di Genova[a], Università di Genova[b], Genova, Italy
P. Chatagnon[a], F. Ferro[a], E. Robutti[a], S. Tosi[a,b]

INFN Sezione di Milano-Bicocca[a], Università di Milano-Bicocca[b], Milano, Italy
A. Benaglia[a], G. Boldrini[a,b], F. Brivio[a], F. Cetorelli[a], F. De Guio[a,b], M.E. Dinardo[a,b], P. Dini[a], S. Gennai[a], R. Gerosa[a,b], A. Ghezzi[a,b], P. Govoni[a,b], L. Guzzi[a], M.T. Lucchini[a,b], M. Malberti[a], S. Malvezzi[a], A. Massironi[a], D. Menasce[a], L. Moroni[a],

M. Paganoni[a,b], D. Pedrini[a], B.S. Pinolini[a], S. Ragazzi[a,b], T. Tabarelli de Fatis[a,b], D. Zuolo[a]

INFN Sezione di Napoli[a], Università di Napoli 'Federico II'[b], Napoli, Italy; Università della Basilicata[c], Potenza, Italy; Scuola Superiore Meridionale (SSM)[d], Napoli, Italy

S. Buontempo[a], A. Cagnotta[a,b], F. Carnevali[a,b], N. Cavallo[a,c], A. De Iorio[a,b], F. Fabozzi[a,c], A.O.M. Iorio[a,b], L. Lista[a,b,54], P. Paolucci[a,34], B. Rossi[a], C. Sciacca[a,b]

INFN Sezione di Padova[a], Università di Padova[b], Padova, Italy; Università di Trento[c], Trento, Italy

R. Ardino[a], P. Azzi[a], N. Bacchetta[a,55], A. Bergnoli[a], M. Biasotto[a,56], P. Bortignon[a], A. Bragagnolo[a,b], R. Carlin[a,b], P. Checchia[a], T. Dorigo[a], F. Gasparini[a,b], G. Grosso[a], L. Layer[a,57], E. Lusiani[a], M. Margoni[a,b], A.T. Meneguzzo[a,b], M. Migliorini[a,b], J. Pazzini[a,b], P. Ronchese[a,b], R. Rossin[a,b], F. Simonetto[a,b], G. Strong[a], M. Tosi[a,b], A. Triossi[a,b], S. Ventura[a], H. Yarar[a,b], M. Zanetti[a,b], P. Zotto[a,b], A. Zucchetta[a,b], G. Zumerle[a,b]

INFN Sezione di Pavia[a], Università di Pavia[b], Pavia, Italy

S. Abu Zeid[a,20], C. Aimè[a,b], A. Braghieri[a], S. Calzaferri[a,b], D. Fiorina[a,b], P. Montagna[a,b], V. Re[a], C. Riccardi[a,b], P. Salvini[a], I. Vai[a,b], P. Vitulo[a,b]

INFN Sezione di Perugia[a], Università di Perugia[b], Perugia, Italy

S. Ajmal[a,b], P. Asenov[a,58], G.M. Bilei[a], D. Ciangottini[a,b], L. Fanò[a,b], M. Magherini[a,b], G. Mantovani[a,b], V. Mariani[a,b], M. Menichelli[a], F. Moscatelli[a,58], A. Piccinelli[a,b], M. Presilla[a,b], A. Rossi[a,b], A. Santocchia[a,b], D. Spiga[a], T. Tedeschi[a,b]

INFN Sezione di Pisa[a], Università di Pisa[b], Scuola Normale Superiore di Pisa[c], Pisa, Italy; Università di Siena[d], Siena, Italy

P. Azzurri[a], G. Bagliesi[a], R. Bhattacharya[a], L. Bianchini[a,b], T. Boccali[a], E. Bossini[a], D. Bruschini[a,c], R. Castaldi[a], M.A. Ciocci[a,b], M. Cipriani[a,b], V. D'Amante[a,d], R. Dell'Orso[a], S. Donato[a], A. Giassi[a], F. Ligabue[a,c], D. Matos Figueiredo[a], A. Messineo[a,b], M. Musich[a,b], F. Palla[a], A. Rizzi[a,b], G. Rolandi[a,c], S. Roy Chowdhury[a], T. Sarkar[a], A. Scribano[a], P. Spagnolo[a], R. Tenchini[a], G. Tonelli[a,b], N. Turini[a,d], A. Venturi[a], P.G. Verdini[a]

INFN Sezione di Roma[a], Sapienza Università di Roma[b], Roma, Italy

P. Barria[a], M. Campana[a,b], F. Cavallari[a], L. Cunqueiro Mendez[a,b], D. Del Re[a,b], E. Di Marco[a], M. Diemoz[a], F. Errico[a,b], E. Longo[a,b], P. Meridiani[a], J. Mijuskovic[a,b], G. Organtini[a,b], F. Pandolfi[a], R. Paramatti[a,b], C. Quaranta[a,b], S. Rahatlou[a,b], C. Rovelli[a], F. Santanastasio[a,b], L. Soffi[a]

INFN Sezione di Torino[a], Università di Torino[b], Torino, Italy; Università del Piemonte Orientale[c], Novara, Italy

N. Amapane[a,b], R. Arcidiacono[a,c], S. Argiro[a,b], M. Arneodo[a,c], N. Bartosik[a], R. Bellan[a,b], A. Bellora[a,b], C. Biino[a], N. Cartiglia[a], M. Costa[a,b], R. Covarelli[a,b],

N. Demaria[a], L. Finco[a], M. Grippo[a,b], B. Kiani[a,b], F. Legger[a], F. Luongo[a,b], C. Mariotti[a], S. Maselli[a], A. Mecca[a,b], E. Migliore[a,b], M. Monteno[a], R. Mulargia[a], M.M. Obertino[a,b], G. Ortona[a], L. Pacher[a,b], N. Pastrone[a], M. Pelliccioni[a], M. Ruspa[a,c], F. Siviero[a,b], V. Sola[a,b], A. Solano[a,b], D. Soldi[a,b], A. Staiano[a], C. Tarricone[a,b], M. Tornago[a,b], D. Trocino[a], G. Umoret[a,b], E. Vlasov[a,b]

INFN Sezione di Trieste[a], Università di Trieste[b], Trieste, Italy
S. Belforte[a], V. Candelise[a,b], M. Casarsa[a], F. Cossutti[a], K. De Leo[a,b], G. Della Ricca[a,b]

Kyungpook National University, Daegu, Korea
S. Dogra, J. Hong, C. Huh, B. Kim, D.H. Kim, J. Kim, H. Lee, S.W. Lee, C.S. Moon, Y.D. Oh, M.S. Ryu, S. Sekmen, Y.C. Yang

Chonnam National University, Institute for Universe and Elementary Particles, Kwangju, Korea
G. Bak, P. Gwak, H. Kim, D.H. Moon

Hanyang University, Seoul, Korea
E. Asilar, D. Kim, T.J. Kim, J.A. Merlin, J. Park

Korea University, Seoul, Korea
S. Choi, S. Han, B. Hong, K. Lee, K.S. Lee, S. Lee, J. Park, S.K. Park, J. Yoo

Kyung Hee University, Department of Physics, Seoul, Korea
J. Goh

Sejong University, Seoul, Korea
H. S. Kim, Y. Kim, S. Lee

Seoul National University, Seoul, Korea
J. Almond, J.H. Bhyun, J. Choi, W. Jun, J. Kim, J.S. Kim, S. Ko, H. Kwon, H. Lee, J. Lee, J. Lee, B.H. Oh, S.B. Oh, H. Seo, U.K. Yang, I. Yoon

University of Seoul, Seoul, Korea
W. Jang, D.Y. Kang, Y. Kang, S. Kim, B. Ko, J.S.H. Lee, Y. Lee, I.C. Park, Y. Roh, I.J. Watson, S. Yang

Yonsei University, Department of Physics, Seoul, Korea
S. Ha, H.D. Yoo

Sungkyunkwan University, Suwon, Korea
M. Choi, M.R. Kim, H. Lee, Y. Lee, I. Yu

College of Engineering and Technology, American University of the Middle East (AUM), Dasman, Kuwait
T. Beyrouthy, Y. Maghrbi

Riga Technical University, Riga, Latvia
K. Dreimanis, A. Gaile, G. Pikurs, A. Potrebko, M. Seidel, V. Veckalns[59]

University of Latvia (LU), Riga, Latvia
N.R. Strautnieks

Vilnius University, Vilnius, Lithuania
M. Ambrozas, A. Juodagalvis, A. Rinkevicius, G. Tamulaitis

National Centre for Particle Physics, Universiti Malaya, Kuala Lumpur, Malaysia
N. Bin Norjoharuddeen, I. Yusuff[60], Z. Zolkapli

Universidad de Sonora (UNISON), Hermosillo, Mexico
J.F. Benitez, A. Castaneda Hernandez, H.A. Encinas Acosta, L.G. Gallegos Maríñez, M. León Coello, J.A. Murillo Quijada, A. Sehrawat, L. Valencia Palomo

Centro de Investigacion y de Estudios Avanzados del IPN, Mexico City, Mexico
G. Ayala, H. Castilla-Valdez, E. De La Cruz-Burelo, I. Heredia-De La Cruz[61], R. Lopez-Fernandez, C.A. Mondragon Herrera, A. Sánchez Hernández

Universidad Iberoamericana, Mexico City, Mexico
C. Oropeza Barrera, M. Ramírez García

Benemerita Universidad Autonoma de Puebla, Puebla, Mexico
I. Bautista, I. Pedraza, H.A. Salazar Ibarguen, C. Uribe Estrada

University of Montenegro, Podgorica, Montenegro
I. Bubanja, N. Raicevic

University of Canterbury, Christchurch, New Zealand
P.H. Butler

National Centre for Physics, Quaid-I-Azam University, Islamabad, Pakistan
A. Ahmad, M.I. Asghar, A. Awais, M.I.M. Awan, H.R. Hoorani, W.A. Khan

AGH University of Krakow, Faculty of Computer Science, Electronics and Telecommunications, Krakow, Poland
V. Avati, L. Grzanka, M. Malawski

National Centre for Nuclear Research, Swierk, Poland
H. Bialkowska, M. Bluj, B. Boimska, M. Górski, M. Kazana, M. Szleper, P. Zalewski

Institute of Experimental Physics, Faculty of Physics, University of Warsaw, Warsaw, Poland
K. Bunkowski, K. Doroba, A. Kalinowski, M. Konecki, J. Krolikowski, A. Muhammad

JHEP10(2024)209

Warsaw University of Technology, Warsaw, Poland
K. Pozniak, W. Zabolotny

Laboratório de Instrumentação e Física Experimental de Partículas, Lisboa, Portugal
M. Araujo, D. Bastos, C. Beirão Da Cruz E Silva, A. Boletti, M. Bozzo, P. Faccioli, M. Gallinaro, J. Hollar, N. Leonardo, T. Niknejad, A. Petrilli, M. Pisano, J. Seixas, J. Varela, J.W. Wulff

Faculty of Physics, University of Belgrade, Belgrade, Serbia
P. Adzic, P. Milenovic

VINCA Institute of Nuclear Sciences, University of Belgrade, Belgrade, Serbia
M. Dordevic, J. Milosevic, V. Rekovic

Centro de Investigaciones Energéticas Medioambientales y Tecnológicas (CIEMAT), Madrid, Spain
M. Aguilar-Benitez, J. Alcaraz Maestre, Cristina F. Bedoya, M. Cepeda, M. Cerrada, N. Colino, B. De La Cruz, A. Delgado Peris, D. Fernández Del Val, J.P. Fernández Ramos, J. Flix, M.C. Fouz, O. Gonzalez Lopez, S. Goy Lopez, J.M. Hernandez, M.I. Josa, J. León Holgado, D. Moran, C. M. Morcillo Perez, Á. Navarro Tobar, C. Perez Dengra, A. Pérez-Calero Yzquierdo, J. Puerta Pelayo, I. Redondo, D.D. Redondo Ferrero, L. Romero, S. Sánchez Navas, L. Urda Gómez, J. Vazquez Escobar, C. Willmott

Universidad Autónoma de Madrid, Madrid, Spain
J.F. de Trocóniz

Universidad de Oviedo, Instituto Universitario de Ciencias y Tecnologías Espaciales de Asturias (ICTEA), Oviedo, Spain
B. Alvarez Gonzalez, J. Cuevas, J. Fernandez Menendez, S. Folgueras, I. Gonzalez Caballero, J.R. González Fernández, E. Palencia Cortezon, C. Ramón Álvarez, V. Rodríguez Bouza, A. Soto Rodríguez, A. Trapote, C. Vico Villalba, P. Vischia

Instituto de Física de Cantabria (IFCA), CSIC-Universidad de Cantabria, Santander, Spain
S. Bhowmik, S. Blanco Fernández, J.A. Brochero Cifuentes, I.J. Cabrillo, A. Calderon, J. Duarte Campderros, M. Fernandez, C. Fernandez Madrazo, G. Gomez, C. Lasaosa García, C. Martinez Rivero, P. Martinez Ruiz del Arbol, F. Matorras, P. Matorras Cuevas, E. Navarrete Ramos, J. Piedra Gomez, L. Scodellaro, I. Vila, J.M. Vizan Garcia

University of Colombo, Colombo, Sri Lanka
M.K. Jayananda, B. Kailasapathy[62], D.U.J. Sonnadara, D.D.C. Wickramarathna

University of Ruhuna, Department of Physics, Matara, Sri Lanka
W.G.D. Dharmaratna, K. Liyanage, N. Perera, N. Wickramage

CERN, European Organization for Nuclear Research, Geneva, Switzerland
D. Abbaneo, C. Amendola, E. Auffray, G. Auzinger, J. Baechler, D. Barney, A. Bermúdez Martínez, M. Bianco, B. Bilin, A.A. Bin Anuar, A. Bocci, E. Brondolin, C. Caillol, T. Camporesi, G. Cerminara, N. Chernyavskaya, D. d'Enterria, A. Dabrowski, A. David, A. De Roeck, M.M. Defranchis, M. Deile, M. Dobson, F. Fallavollita[63], L. Forthomme, G. Franzoni, W. Funk, S. Giani, D. Gigi, K. Gill, F. Glege, L. Gouskos, M. Haranko, J. Hegeman, B. Huber, V. Innocente, T. James, P. Janot, J. Kieseler, S. Laurila, P. Lecoq, E. Leutgeb, C. Lourenço, B. Maier, L. Malgeri, M. Mannelli, A.C. Marini, M. Matthewman, F. Meijers, S. Mersi, E. Meschi, V. Milosevic, F. Moortgat, M. Mulders, S. Orfanelli, F. Pantaleo, M. Peruzzi, G. Petrucciani, A. Pfeiffer, M. Pierini, D. Piparo, H. Qu, D. Rabady, G. Reales Gutiérrez, M. Rovere, H. Sakulin, S. Scarfi, C. Schwick, M. Selvaggi, A. Sharma, K. Shchelina, P. Silva, P. Sphicas[64], A.G. Stahl Leiton, A. Steen, S. Summers, D. Treille, P. Tropea, A. Tsirou, D. Walter, J. Wanczyk[65], K.A. Wozniak[66], P. Zehetner, P. Zejdl, W.D. Zeuner

Paul Scherrer Institut, Villigen, Switzerland
T. Bevilacqua[67], L. Caminada[67], A. Ebrahimi, W. Erdmann, R. Horisberger, Q. Ingram, H.C. Kaestli, D. Kotlinski, C. Lange, M. Missiroli[67], L. Noehte[67], T. Rohe

ETH Zurich - Institute for Particle Physics and Astrophysics (IPA), Zurich, Switzerland
T.K. Aarrestad, K. Androsov[65], M. Backhaus, A. Calandri, C. Cazzaniga, K. Datta, A. De Cosa, G. Dissertori, M. Dittmar, M. Donegà, F. Eble, M. Galli, K. Gedia, F. Glessgen, C. Grab, D. Hits, W. Lustermann, A.-M. Lyon, R.A. Manzoni, M. Marchegiani, L. Marchese, C. Martin Perez, A. Mascellani[65], F. Nessi-Tedaldi, F. Pauss, V. Perovic, S. Pigazzini, M.G. Ratti, M. Reichmann, C. Reissel, T. Reitenspiess, B. Ristic, F. Riti, D. Ruini, D.A. Sanz Becerra, R. Seidita, J. Steggemann[65], D. Valsecchi, R. Wallny

Universität Zürich, Zurich, Switzerland
C. Amsler[68], P. Bärtschi, C. Botta, D. Brzhechko, M.F. Canelli, K. Cormier, R. Del Burgo, J.K. Heikkilä, M. Huwiler, W. Jin, A. Jofrehei, B. Kilminster, S. Leontsinis, S.P. Liechti, A. Macchiolo, P. Meiring, V.M. Mikuni, U. Molinatti, I. Neutelings, A. Reimers, P. Robmann, S. Sanchez Cruz, K. Schweiger, M. Senger, Y. Takahashi, R. Tramontano

National Central University, Chung-Li, Taiwan
C. Adloff[69], C.M. Kuo, W. Lin, P.K. Rout, P.C. Tiwari[44], S.S. Yu

National Taiwan University (NTU), Taipei, Taiwan
L. Ceard, Y. Chao, K.F. Chen, P.s. Chen, Z.g. Chen, W.-S. Hou, T.h. Hsu, Y.w. Kao, R. Khurana, G. Kole, Y.y. Li, R.-S. Lu, E. Paganis, A. Psallidas, X.f. Su, J. Thomas-Wilsker, L.s. Tsai, H.y. Wu, E. Yazgan

JHEP10(2024)209

High Energy Physics Research Unit, Department of Physics, Faculty of Science, Chulalongkorn University, Bangkok, Thailand
C. Asawatangtrakuldee, N. Srimanobhas, V. Wachirapusitanand

Çukurova University, Physics Department, Science and Art Faculty, Adana, Turkey
D. Agyel, F. Boran, Z.S. Demiroglu, F. Dolek, I. Dumanoglu[70], E. Eskut, Y. Guler[71], E. Gurpinar Guler[71], C. Isik, O. Kara, A. Kayis Topaksu, U. Kiminsu, G. Onengut, K. Ozdemir[72], A. Polatoz, B. Tali[73], U.G. Tok, S. Turkcapar, E. Uslan, I.S. Zorbakir

Middle East Technical University, Physics Department, Ankara, Turkey
M. Yalvac[74]

Bogazici University, Istanbul, Turkey
B. Akgun, I.O. Atakisi, E. Gülmez, M. Kaya[75], O. Kaya[76], S. Tekten[77]

Istanbul Technical University, Istanbul, Turkey
A. Cakir, K. Cankocak[70,78], Y. Komurcu, S. Sen[79]

Istanbul University, Istanbul, Turkey
O. Aydilek, S. Cerci[73], V. Epshteyn, B. Hacisahinoglu, I. Hos[80], B. Isildak[81], B. Kaynak, S. Ozkorucuklu, O. Potok, H. Sert, C. Simsek, D. Sunar Cerci[73], C. Zorbilmez

Institute for Scintillation Materials of National Academy of Science of Ukraine, Kharkiv, Ukraine
A. Boyaryntsev, B. Grynyov

National Science Centre, Kharkiv Institute of Physics and Technology, Kharkiv, Ukraine
L. Levchuk

University of Bristol, Bristol, United Kingdom
D. Anthony, J.J. Brooke, A. Bundock, F. Bury, E. Clement, D. Cussans, H. Flacher, M. Glowacki, J. Goldstein, H.F. Heath, L. Kreczko, B. Krikler, S. Paramesvaran, S. Seif El Nasr-Storey, V.J. Smith, N. Stylianou[82], K. Walkingshaw Pass, R. White

Rutherford Appleton Laboratory, Didcot, United Kingdom
A.H. Ball, K.W. Bell, A. Belyaev[83], C. Brew, R.M. Brown, D.J.A. Cockerill, C. Cooke, K.V. Ellis, K. Harder, S. Harper, M.-L. Holmberg[84], J. Linacre, K. Manolopoulos, D.M. Newbold, E. Olaiya, D. Petyt, T. Reis, G. Salvi, T. Schuh, C.H. Shepherd-Themistocleous, I.R. Tomalin, T. Williams

Imperial College, London, United Kingdom
R. Bainbridge, P. Bloch, C.E. Brown, O. Buchmuller, V. Cacchio, C.A. Carrillo Montoya, G.S. Chahal[85], D. Colling, J.S. Dancu, P. Dauncey, G. Davies, J. Davies, M. Della Negra,

S. Fayer, G. Fedi, G. Hall, M.H. Hassanshahi, A. Howard, G. Iles, M. Knight, J. Langford, L. Lyons, A.-M. Magnan, S. Malik, A. Martelli, M. Mieskolainen, J. Nash[86], M. Pesaresi, B.C. Radburn-Smith, A. Richards, A. Rose, C. Seez, R. Shukla, A. Tapper, K. Uchida, G.P. Uttley, L.H. Vage, T. Virdee[34], M. Vojinovic, N. Wardle, D. Winterbottom

Brunel University, Uxbridge, United Kingdom
K. Coldham, J.E. Cole, A. Khan, P. Kyberd, I.D. Reid

Baylor University, Waco, Texas, U.S.A.
S. Abdullin, A. Brinkerhoff, B. Caraway, J. Dittmann, K. Hatakeyama, J. Hiltbrand, A.R. Kanuganti, B. McMaster, M. Saunders, S. Sawant, C. Sutantawibul, M. Toms[87], J. Wilson

Catholic University of America, Washington, DC, U.S.A.
R. Bartek, A. Dominguez, C. Huerta Escamilla, A.E. Simsek, R. Uniyal, A.M. Vargas Hernandez

The University of Alabama, Tuscaloosa, Alabama, U.S.A.
R. Chudasama, S.I. Cooper, S.V. Gleyzer, C.U. Perez, P. Rumerio[88], E. Usai, C. West, R. Yi

Boston University, Boston, Massachusetts, U.S.A.
A. Akpinar, A. Albert, D. Arcaro, C. Cosby, Z. Demiragli, C. Erice, E. Fontanesi, D. Gastler, S. Jeon, J. Rohlf, K. Salyer, D. Sperka, D. Spitzbart, I. Suarez, A. Tsatsos, S. Yuan

Brown University, Providence, Rhode Island, U.S.A.
G. Benelli, X. Coubez[29], D. Cutts, M. Hadley, U. Heintz, J.M. Hogan[89], T. Kwon, G. Landsberg, K.T. Lau, D. Li, J. Luo, S. Mondal, M. Narain[†], N. Pervan, S. Sagir[90], F. Simpson, M. Stamenkovic, W.Y. Wong, X. Yan, W. Zhang

University of California, Davis, Davis, California, U.S.A.
S. Abbott, J. Bonilla, C. Brainerd, R. Breedon, M. Calderon De La Barca Sanchez, M. Chertok, M. Citron, J. Conway, P.T. Cox, R. Erbacher, F. Jensen, O. Kukral, G. Mocellin, M. Mulhearn, D. Pellett, W. Wei, Y. Yao, F. Zhang

University of California, Los Angeles, California, U.S.A.
M. Bachtis, R. Cousins, A. Datta, J. Hauser, M. Ignatenko, M.A. Iqbal, T. Lam, E. Manca, W.A. Nash, D. Saltzberg, B. Stone, V. Valuev

University of California, Riverside, Riverside, California, U.S.A.
R. Clare, M. Gordon, G. Hanson, W. Si, S. Wimpenny[†]

University of California, San Diego, La Jolla, California, U.S.A.
J.G. Branson, S. Cittolin, S. Cooperstein, D. Diaz, J. Duarte, L. Giannini, J. Guiang, R. Kansal, V. Krutelyov, R. Lee, J. Letts, M. Masciovecchio, F. Mokhtar, M. Pieri,

JHEP10(2024)209

M. Quinnan, B.V. Sathia Narayanan, V. Sharma, M. Tadel, E. Vourliotis, F. Würthwein, Y. Xiang, A. Yagil

University of California, Santa Barbara - Department of Physics, Santa Barbara, California, U.S.A.

A. Barzdukas, L. Brennan, C. Campagnari, G. Collura, A. Dorsett, J. Incandela, M. Kilpatrick, J. Kim, A.J. Li, P. Masterson, H. Mei, M. Oshiro, J. Richman, U. Sarica, R. Schmitz, F. Setti, J. Sheplock, D. Stuart, S. Wang

California Institute of Technology, Pasadena, California, U.S.A.

A. Bornheim, O. Cerri, A. Latorre, J.M. Lawhorn, J. Mao, H.B. Newman, T. Q. Nguyen, M. Spiropulu, J.R. Vlimant, C. Wang, S. Xie, R.Y. Zhu

Carnegie Mellon University, Pittsburgh, Pennsylvania, U.S.A.

J. Alison, S. An, M.B. Andrews, P. Bryant, V. Dutta, T. Ferguson, A. Harilal, C. Liu, T. Mudholkar, S. Murthy, M. Paulini, A. Roberts, A. Sanchez, W. Terrill

University of Colorado Boulder, Boulder, Colorado, U.S.A.

J.P. Cumalat, W.T. Ford, A. Hassani, G. Karathanasis, E. MacDonald, N. Manganelli, F. Marini, A. Perloff, C. Savard, N. Schonbeck, K. Stenson, K.A. Ulmer, S.R. Wagner, N. Zipper

Cornell University, Ithaca, New York, U.S.A.

J. Alexander, S. Bright-Thonney, X. Chen, D.J. Cranshaw, J. Fan, X. Fan, D. Gadkari, S. Hogan, J. Monroy, J.R. Patterson, J. Reichert, M. Reid, A. Ryd, J. Thom, P. Wittich, R. Zou

Fermi National Accelerator Laboratory, Batavia, Illinois, U.S.A.

M. Albrow, M. Alyari, O. Amram, G. Apollinari, A. Apresyan, L.A.T. Bauerdick, D. Berry, J. Berryhill, P.C. Bhat, K. Burkett, J.N. Butler, A. Canepa, G.B. Cerati, H.W.K. Cheung, F. Chlebana, G. Cummings, J. Dickinson, I. Dutta, V.D. Elvira, Y. Feng, J. Freeman, A. Gandrakota, Z. Gecse, L. Gray, D. Green, A. Grummer, S. Grünendahl, D. Guerrero, O. Gutsche, R.M. Harris, R. Heller, T.C. Herwig, J. Hirschauer, L. Horyn, B. Jayatilaka, S. Jindariani, M. Johnson, U. Joshi, T. Klijnsma, B. Klima, K.H.M. Kwok, S. Lammel, D. Lincoln, R. Lipton, T. Liu, C. Madrid, K. Maeshima, C. Mantilla, D. Mason, P. McBride, P. Merkel, S. Mrenna, S. Nahn, J. Ngadiuba, D. Noonan, V. Papadimitriou, N. Pastika, K. Pedro, C. Pena[91], F. Ravera, A. Reinsvold Hall[92], L. Ristori, E. Sexton-Kennedy, N. Smith, A. Soha, L. Spiegel, S. Stoynev, J. Strait, L. Taylor, S. Tkaczyk, N.V. Tran, L. Uplegger, E.W. Vaandering, I. Zoi

University of Florida, Gainesville, Florida, U.S.A.

C. Aruta, P. Avery, D. Bourilkov, L. Cadamuro, P. Chang, V. Cherepanov, R.D. Field, E. Koenig, M. Kolosova, J. Konigsberg, A. Korytov, K.H. Lo, K. Matchev, N. Menendez, G. Mitselmakher, K. Mohrman, A. Muthirakalayil Madhu, N. Rawal, D. Rosenzweig, S. Rosenzweig, K. Shi, J. Wang

Florida State University, Tallahassee, Florida, U.S.A.
T. Adams, A. Al Kadhim, A. Askew, N. Bower, R. Habibullah, V. Hagopian, R. Hashmi, R.S. Kim, S. Kim, T. Kolberg, G. Martinez, H. Prosper, P.R. Prova, O. Viazlo, M. Wulansatiti, R. Yohay, J. Zhang

Florida Institute of Technology, Melbourne, Florida, U.S.A.
B. Alsufyani, M.M. Baarmand, S. Butalla, T. Elkafrawy[20], M. Hohlmann, R. Kumar Verma, M. Rahmani

University of Illinois Chicago, Chicago, U.S.A., Chicago, U.S.A.
M.R. Adams, C. Bennett, R. Cavanaugh, S. Dittmer, R. Escobar Franco, O. Evdokimov, C.E. Gerber, D.J. Hofman, J.h. Lee, D. S. Lemos, A.H. Merrit, C. Mills, S. Nanda, G. Oh, B. Ozek, D. Pilipovic, T. Roy, S. Rudrabhatla, M.B. Tonjes, N. Varelas, X. Wang, Z. Ye, J. Yoo

The University of Iowa, Iowa City, Iowa, U.S.A.
M. Alhusseini, D. Blend, K. Dilsiz[93], L. Emediato, G. Karaman, O.K. Köseyan, J.-P. Merlo, A. Mestvirishvili[94], J. Nachtman, O. Neogi, H. Ogul[95], Y. Onel, A. Penzo, C. Snyder, E. Tiras[96]

Johns Hopkins University, Baltimore, Maryland, U.S.A.
B. Blumenfeld, L. Corcodilos, J. Davis, A.V. Gritsan, L. Kang, S. Kyriacou, P. Maksimovic, M. Roguljic, J. Roskes, S. Sekhar, M. Swartz, T.Á. Vámi

The University of Kansas, Lawrence, Kansas, U.S.A.
A. Abreu, L.F. Alcerro Alcerro, J. Anguiano, P. Baringer, A. Bean, Z. Flowers, D. Grove, J. King, G. Krintiras, M. Lazarovits, C. Le Mahieu, C. Lindsey, J. Marquez, N. Minafra, M. Murray, M. Nickel, M. Pitt, S. Popescu[97], C. Rogan, C. Royon, R. Salvatico, S. Sanders, C. Smith, Q. Wang, G. Wilson

Kansas State University, Manhattan, Kansas, U.S.A.
B. Allmond, A. Ivanov, K. Kaadze, A. Kalogeropoulos, D. Kim, Y. Maravin, K. Nam, J. Natoli, D. Roy, G. Sorrentino

Lawrence Livermore National Laboratory, Livermore, California, U.S.A.
F. Rebassoo, D. Wright

University of Maryland, College Park, Maryland, U.S.A.
E. Adams, A. Baden, O. Baron, A. Belloni, A. Bethani, Y.M. Chen, S.C. Eno, N.J. Hadley, S. Jabeen, R.G. Kellogg, T. Koeth, Y. Lai, S. Lascio, A.C. Mignerey, S. Nabili, C. Palmer, C. Papageorgakis, M.M. Paranjpe, L. Wang, K. Wong

Massachusetts Institute of Technology, Cambridge, Massachusetts, U.S.A.
J. Bendavid, W. Busza, I.A. Cali, Y. Chen, M. D'Alfonso, J. Eysermans, C. Freer, G. Gomez-Ceballos, M. Goncharov, P. Harris, D. Hoang, D. Kovalskyi, J. Krupa, L. Lavezzo,

Y.-J. Lee, K. Long, C. Mironov, C. Paus, D. Rankin, C. Roland, G. Roland, S. Rothman, Z. Shi, G.S.F. Stephans, J. Wang, Z. Wang, B. Wyslouch, T. J. Yang

University of Minnesota, Minneapolis, Minnesota, U.S.A.
B. Crossman, B.M. Joshi, C. Kapsiak, M. Krohn, D. Mahon, J. Mans, B. Marzocchi, S. Pandey, M. Revering, R. Rusack, R. Saradhy, N. Schroeder, N. Strobbe, M.A. Wadud

University of Mississippi, Oxford, Mississippi, U.S.A.
L.M. Cremaldi

University of Nebraska-Lincoln, Lincoln, Nebraska, U.S.A.
K. Bloom, M. Bryson, D.R. Claes, C. Fangmeier, F. Golf, G. Haza, J. Hossain, C. Joo, I. Kravchenko, I. Reed, J.E. Siado, W. Tabb, A. Vagnerini, A. Wightman, F. Yan, D. Yu, A.G. Zecchinelli

State University of New York at Buffalo, Buffalo, New York, U.S.A.
G. Agarwal, H. Bandyopadhyay, L. Hay, I. Iashvili, A. Kharchilava, C. McLean, M. Morris, D. Nguyen, S. Rappoccio, H. Rejeb Sfar, A. Williams

Northeastern University, Boston, Massachusetts, U.S.A.
G. Alverson, E. Barberis, Y. Haddad, Y. Han, A. Krishna, J. Li, M. Lu, G. Madigan, R. Mccarthy, D.M. Morse, V. Nguyen, T. Orimoto, A. Parker, L. Skinnari, A. Tishelman-Charny, B. Wang, D. Wood

Northwestern University, Evanston, Illinois, U.S.A.
S. Bhattacharya, J. Bueghly, Z. Chen, K.A. Hahn, Y. Liu, Y. Miao, D.G. Monk, M.H. Schmitt, A. Taliercio, M. Velasco

University of Notre Dame, Notre Dame, Indiana, U.S.A.
R. Band, R. Bucci, S. Castells, M. Cremonesi, A. Das, R. Goldouzian, M. Hildreth, K.W. Ho, K. Hurtado Anampa, C. Jessop, K. Lannon, J. Lawrence, N. Loukas, L. Lutton, J. Mariano, N. Marinelli, I. Mcalister, T. McCauley, C. Mcgrady, C. Moore, Y. Musienko[16], H. Nelson, M. Osherson, R. Ruchti, A. Townsend, M. Wayne, H. Yockey, M. Zarucki, L. Zygala

The Ohio State University, Columbus, Ohio, U.S.A.
A. Basnet, B. Bylsma, M. Carrigan, L.S. Durkin, C. Hill, M. Joyce, A. Lesauvage, M. Nunez Ornelas, K. Wei, B.L. Winer, B. R. Yates

Princeton University, Princeton, New Jersey, U.S.A.
F.M. Addesa, H. Bouchamaoui, P. Das, G. Dezoort, P. Elmer, A. Frankenthal, B. Greenberg, N. Haubrich, S. Higginbotham, G. Kopp, S. Kwan, D. Lange, A. Loeliger, D. Marlow, I. Ojalvo, J. Olsen, A. Shevelev, D. Stickland, C. Tully

University of Puerto Rico, Mayaguez, Puerto Rico, U.S.A.
S. Malik

JHEP10(2024)209

Purdue University, West Lafayette, Indiana, U.S.A.
A.S. Bakshi, V.E. Barnes, S. Chandra, R. Chawla, S. Das, A. Gu, L. Gutay, M. Jones, A.W. Jung, D. Kondratyev, A.M. Koshy, M. Liu, G. Negro, N. Neumeister, G. Paspalaki, S. Piperov, V. Scheurer, J.F. Schulte, M. Stojanovic, J. Thieman, A. K. Virdi, F. Wang, W. Xie

Purdue University Northwest, Hammond, Indiana, U.S.A.
J. Dolen, N. Parashar, A. Pathak

Rice University, Houston, Texas, U.S.A.
D. Acosta, A. Baty, T. Carnahan, S. Dildick, K.M. Ecklund, P.J. Fernández Manteca, S. Freed, P. Gardner, F.J.M. Geurts, A. Kumar, W. Li, O. Miguel Colin, B.P. Padley, R. Redjimi, J. Rotter, E. Yigitbasi, Y. Zhang

University of Rochester, Rochester, New York, U.S.A.
A. Bodek, P. de Barbaro, R. Demina, J.L. Dulemba, C. Fallon, A. Garcia-Bellido, O. Hindrichs, A. Khukhunaishvili, P. Parygin[87], E. Popova[87], R. Taus, G.P. Van Onsem

The Rockefeller University, New York, New York, U.S.A.
K. Goulianos

Rutgers, The State University of New Jersey, Piscataway, New Jersey, U.S.A.
B. Chiarito, J.P. Chou, Y. Gershtein, E. Halkiadakis, A. Hart, M. Heindl, D. Jaroslawski, O. Karacheban[32], I. Laflotte, A. Lath, R. Montalvo, K. Nash, H. Routray, S. Salur, S. Schnetzer, S. Somalwar, R. Stone, S.A. Thayil, S. Thomas, J. Vora, H. Wang

University of Tennessee, Knoxville, Tennessee, U.S.A.
H. Acharya, D. Ally, A.G. Delannoy, S. Fiorendi, T. Holmes, N. Karunarathna, L. Lee, E. Nibigira, S. Spanier

Texas A&M University, College Station, Texas, U.S.A.
D. Aebi, M. Ahmad, O. Bouhali[98], M. Dalchenko, R. Eusebi, J. Gilmore, T. Huang, T. Kamon[99], H. Kim, S. Luo, S. Malhotra, R. Mueller, D. Overton, D. Rathjens, A. Safonov

Texas Tech University, Lubbock, Texas, U.S.A.
N. Akchurin, J. Damgov, V. Hegde, A. Hussain, Y. Kazhykarim, K. Lamichhane, S.W. Lee, A. Mankel, T. Mengke, S. Muthumuni, T. Peltola, I. Volobouev, A. Whitbeck

Vanderbilt University, Nashville, Tennessee, U.S.A.
E. Appelt, S. Greene, A. Gurrola, W. Johns, R. Kunnawalkam Elayavalli, A. Melo, F. Romeo, P. Sheldon, S. Tuo, J. Velkovska, J. Viinikainen

University of Virginia, Charlottesville, Virginia, U.S.A.
B. Cardwell, B. Cox, J. Hakala, R. Hirosky, A. Ledovskoy, A. Li, C. Neu, C.E. Perez Lara

JHEP10(2024)209

Wayne State University, Detroit, Michigan, U.S.A.
P.E. Karchin

University of Wisconsin - Madison, Madison, Wisconsin, U.S.A.
A. Aravind, S. Banerjee, K. Black, T. Bose, S. Dasu, I. De Bruyn, P. Everaerts, C. Galloni, H. He, M. Herndon, A. Herve, C.K. Koraka, A. Lanaro, R. Loveless, J. Madhusudanan Sreekala, A. Mallampalli, A. Mohammadi, S. Mondal, G. Parida, D. Pinna, A. Savin, V. Shang, V. Sharma, W.H. Smith, D. Teague, H.F. Tsoi, W. Vetens, A. Warden

Authors affiliated with an institute or an international laboratory covered by a cooperation agreement with CERN
S. Afanasiev, V. Andreev, Yu. Andreev, T. Aushev, M. Azarkin, A. Babaev, A. Belyaev, V. Blinov[100], E. Boos, V. Borshch, D. Budkouski, V. Bunichev, M. Chadeeva[100], V. Chekhovsky, M. Danilov[100], A. Dermenev, T. Dimova[100], D. Druzhkin[101], M. Dubinin[91], L. Dudko, G. Gavrilov, V. Gavrilov, S. Gninenko, V. Golovtcov, N. Golubev, I. Golutvin, I. Gorbunov, A. Gribushin, Y. Ivanov, V. Kachanov, L. Kardapoltsev[100], V. Karjavine, A. Karneyeu, V. Kim[100], M. Kirakosyan, D. Kirpichnikov, M. Kirsanov, V. Klyukhin, O. Kodolova[102], D. Konstantinov, V. Korenkov, A. Kozyrev[100], N. Krasnikov, A. Lanev, P. Levchenko[103], O. Lukina, N. Lychkovskaya, V. Makarenko, A. Malakhov, V. Matveev[100], V. Murzin, A. Nikitenko[104,102], S. Obraztsov, V. Oreshkin, V. Palichik, V. Perelygin, S. Petrushanko, S. Polikarpov[100], V. Popov, O. Radchenko[100], M. Savina, V. Savrin, V. Shalaev, S. Shmatov, S. Shulha, Y. Skovpen[100], S. Slabospitskii, V. Smirnov, A. Snigirev, D. Sosnov, V. Sulimov, E. Tcherniaev, A. Terkulov, O. Teryaev, I. Tlisova, A. Toropin, L. Uvarov, A. Uzunian, A. Vorobyev[†], N. Voytishin, B.S. Yuldashev[105], A. Zarubin, I. Zhizhin, A. Zhokin

[†] *Deceased*
[1] *Also at Yerevan State University, Yerevan, Armenia*
[2] *Also at TU Wien, Vienna, Austria*
[3] *Also at Institute of Basic and Applied Sciences, Faculty of Engineering, Arab Academy for Science, Technology and Maritime Transport, Alexandria, Egypt*
[4] *Also at Ghent University, Ghent, Belgium*
[5] *Also at Universidade Estadual de Campinas, Campinas, Brazil*
[6] *Also at Federal University of Rio Grande do Sul, Porto Alegre, Brazil*
[7] *Also at UFMS, Nova Andradina, Brazil*
[8] *Also at Nanjing Normal University, Nanjing, China*
[9] *Now at Henan Normal University, Xinxiang, China*
[10] *Now at The University of Iowa, Iowa City, Iowa, U.S.A.*
[11] *Also at University of Chinese Academy of Sciences, Beijing, China*
[12] *Also at China Center of Advanced Science and Technology, Beijing, China*
[13] *Also at University of Chinese Academy of Sciences, Beijing, China*
[14] *Also at China Spallation Neutron Source, Guangdong, China*
[15] *Also at Université Libre de Bruxelles, Bruxelles, Belgium*
[16] *Also at an institute or an international laboratory covered by a cooperation agreement with CERN*
[17] *Also at Helwan University, Cairo, Egypt*
[18] *Now at Zewail City of Science and Technology, Zewail, Egypt*

JHEP10(2024)209

[19] *Also at British University in Egypt, Cairo, Egypt*
[20] *Now at Ain Shams University, Cairo, Egypt*
[21] *Also at Birla Institute of Technology, Mesra, Mesra, India*
[22] *Also at Purdue University, West Lafayette, Indiana, U.S.A.*
[23] *Also at Université de Haute Alsace, Mulhouse, France*
[24] *Also at Department of Physics, Tsinghua University, Beijing, China*
[25] *Also at Tbilisi State University, Tbilisi, Georgia*
[26] *Also at The University of the State of Amazonas, Manaus, Brazil*
[27] *Also at Erzincan Binali Yildirim University, Erzincan, Turkey*
[28] *Also at University of Hamburg, Hamburg, Germany*
[29] *Also at RWTH Aachen University, III. Physikalisches Institut A, Aachen, Germany*
[30] *Also at Isfahan University of Technology, Isfahan, Iran*
[31] *Also at Bergische University Wuppertal (BUW), Wuppertal, Germany*
[32] *Also at Brandenburg University of Technology, Cottbus, Germany*
[33] *Also at Forschungszentrum Jülich, Juelich, Germany*
[34] *Also at CERN, European Organization for Nuclear Research, Geneva, Switzerland*
[35] *Also at Institute of Physics, University of Debrecen, Debrecen, Hungary*
[36] *Also at Institute of Nuclear Research ATOMKI, Debrecen, Hungary*
[37] *Now at Universitatea Babes-Bolyai - Facultatea de Fizica, Cluj-Napoca, Romania*
[38] *Also at Physics Department, Faculty of Science, Assiut University, Assiut, Egypt*
[39] *Also at HUN-REN Wigner Research Centre for Physics, Budapest, Hungary*
[40] *Also at Faculty of Informatics, University of Debrecen, Debrecen, Hungary*
[41] *Also at Punjab Agricultural University, Ludhiana, India*
[42] *Also at University of Hyderabad, Hyderabad, India*
[43] *Also at University of Visva-Bharati, Santiniketan, India*
[44] *Also at Indian Institute of Science (IISc), Bangalore, India*
[45] *Also at IIT Bhubaneswar, Bhubaneswar, India*
[46] *Also at Institute of Physics, Bhubaneswar, India*
[47] *Also at Deutsches Elektronen-Synchrotron, Hamburg, Germany*
[48] *Also at Department of Physics, Isfahan University of Technology, Isfahan, Iran*
[49] *Also at Sharif University of Technology, Tehran, Iran*
[50] *Also at Department of Physics, University of Science and Technology of Mazandaran, Behshahr, Iran*
[51] *Also at Italian National Agency for New Technologies, Energy and Sustainable Economic Development, Bologna, Italy*
[52] *Also at Centro Siciliano di Fisica Nucleare e di Struttura Della Materia, Catania, Italy*
[53] *Also at Università degli Studi Guglielmo Marconi, Roma, Italy*
[54] *Also at Scuola Superiore Meridionale, Università di Napoli 'Federico II', Napoli, Italy*
[55] *Also at Fermi National Accelerator Laboratory, Batavia, Illinois, U.S.A.*
[56] *Also at Laboratori Nazionali di Legnaro dell'INFN, Legnaro, Italy*
[57] *Also at Università di Napoli 'Federico II', Napoli, Italy*
[58] *Also at Consiglio Nazionale delle Ricerche - Istituto Officina dei Materiali, Perugia, Italy*
[59] *Also at Riga Technical University, Riga, Latvia*
[60] *Also at Department of Applied Physics, Faculty of Science and Technology, Universiti Kebangsaan Malaysia, Bangi, Malaysia*
[61] *Also at Consejo Nacional de Ciencia y Tecnología, Mexico City, Mexico*
[62] *Also at Trincomalee Campus, Eastern University, Sri Lanka, Nilaveli, Sri Lanka*
[63] *Also at INFN Sezione di Pavia, Università di Pavia, Pavia, Italy*
[64] *Also at National and Kapodistrian University of Athens, Athens, Greece*
[65] *Also at Ecole Polytechnique Fédérale Lausanne, Lausanne, Switzerland*
[66] *Also at University of Vienna Faculty of Computer Science, Vienna, Austria*
[67] *Also at Universität Zürich, Zurich, Switzerland*
[68] *Also at Stefan Meyer Institute for Subatomic Physics, Vienna, Austria*
[69] *Also at Laboratoire d'Annecy-le-Vieux de Physique des Particules, IN2P3-CNRS, Annecy-le-Vieux, France*

JHEP10(2024)209

[70] Also at Near East University, Research Center of Experimental Health Science, Mersin, Turkey
[71] Also at Konya Technical University, Konya, Turkey
[72] Also at Izmir Bakircay University, Izmir, Turkey
[73] Also at Adiyaman University, Adiyaman, Turkey
[74] Also at Bozok Universitetesi Rektörlügü, Yozgat, Turkey
[75] Also at Marmara University, Istanbul, Turkey
[76] Also at Milli Savunma University, Istanbul, Turkey
[77] Also at Kafkas University, Kars, Turkey
[78] Now at stanbul Okan University, Istanbul, Turkey
[79] Also at Hacettepe University, Ankara, Turkey
[80] Also at Istanbul University - Cerrahpasa, Faculty of Engineering, Istanbul, Turkey
[81] Also at Yildiz Technical University, Istanbul, Turkey
[82] Also at Vrije Universiteit Brussel, Brussel, Belgium
[83] Also at School of Physics and Astronomy, University of Southampton, Southampton, United Kingdom
[84] Also at University of Bristol, Bristol, United Kingdom
[85] Also at IPPP Durham University, Durham, United Kingdom
[86] Also at Monash University, Faculty of Science, Clayton, Australia
[87] Now at an institute or an international laboratory covered by a cooperation agreement with CERN
[88] Also at Università di Torino, Torino, Italy
[89] Also at Bethel University, St. Paul, Minnesota, U.S.A.
[90] Also at Karamanoğlu Mehmetbey University, Karaman, Turkey
[91] Also at California Institute of Technology, Pasadena, California, U.S.A.
[92] Also at United States Naval Academy, Annapolis, Maryland, U.S.A.
[93] Also at Bingol University, Bingol, Turkey
[94] Also at Georgian Technical University, Tbilisi, Georgia
[95] Also at Sinop University, Sinop, Turkey
[96] Also at Erciyes University, Kayseri, Turkey
[97] Also at Horia Hulubei National Institute of Physics and Nuclear Engineering (IFIN-HH), Bucharest, Romania
[98] Also at Texas A&M University at Qatar, Doha, Qatar
[99] Also at Kyungpook National University, Daegu, Korea
[100] Also at another institute or international laboratory covered by a cooperation agreement with CERN
[101] Also at Universiteit Antwerpen, Antwerpen, Belgium
[102] Also at Yerevan Physics Institute, Yerevan, Armenia
[103] Also at Northeastern University, Boston, Massachusetts, U.S.A.
[104] Also at Imperial College, London, United Kingdom
[105] Also at Institute of Nuclear Physics of the Uzbekistan Academy of Sciences, Tashkent, Uzbekistan

JHEP10(2024)209